NTNU

Norwegian University of
Science and Technology

Study of a Graphite Sensor for Alumina Concentration Measurements in Cryolite Melts

Karoline Aasen Nilsen

Chemical Engineering and Biotechnology
Submission date: June 2018
Supervisor: Espen Sandnes, IMA
Co-supervisor: Gisle Øye, IKP

Norwegian University of Science and Technology
Department of Materials Science and Engineering

Think like a proton and stay positive

Preface

This master thesis constitute the final work of my five year Master of Science studies in Chemical Engineering at the Norwegian University of Technology and Science (NTNU). I am very grateful to have had this opportunity, and I am certain that what I have learned during this working period will benefit me later.

First of all, I will like to give a special thank to my supervisor Espen Sandnes and Gisle Øye who gave me the opportunity to write a thesis within primary aluminium production. Espen Sandnes, your engagement, encouragement and valuable discussions have been very much appreciated.

Secondly I will like to thank Christian Rosenkilde, at Hydro, for great ideas and educational discussions and Luis Bracamonte for his help with the experimental work and for always being positive.

I would also like to thank Henrik Gudbrandsen his essential help in the laboratory and for helpful response to my questions.

Finally I would like to thank Aksel Alstad at the NTNU mechanical workshop for machining and assembling all of my electrodes and for always being in such a good mood.

Thank you for taking the time to read through my thesis, I hope you enjoy!

Summary

Alumina dissolution is one of the most crucial processes taking place in the Hall-Héroult process for the production of primary aluminium. One of the key issues for advanced aluminium electrolysis is therefore to understand and improve the dissolution process. In order to understand it, it is important to have a method for which the alumina concentration can be measured. The literature describes several methods that have been tested. Electromotive force, emf, measurements is one of the methods. In this thesis electromotive force measurements between a graphite sensor and two difference reference electrodes (alumina reference electrode and graphite reference electrode) have been studied in order to figure out if graphite material is suited for determination of alumina concentration in cryolite melts.

The results showed a decreasing trend in emf values when alumina was added as expected from theoretical calculation. An important observation from the initial experiments was that it was observed sudden drops and jumps in emf immediately after addition. These drops and jumps are probably due to other changes in the system and a large part of the following work was dedicated to reveal the reasons for this behaviour.

Immediate changes in emf in the moment alumina was added may be due to air which flowed together with the powder down to the melt and caused an immediate change of the potential on the graphite sensor due to the formation of CO and CO_2. Introduction of CO_2 gas to the system gave substantial impact on the emf. So the assumption of a constant partial pressure of CO/CO_2 used in the theoretical calculations of potential might not be valid, and a solid buffer system of CO/CO_2 may be needed to reduce the influence of variation in the partial pressures of CO and CO_2. However, the sudden drops and jumps in the potential after alumina addition were still present even though CO_2 was fed to the system.

It seemed like gas evolution caused by the reaction between moisture or hydoxyl containing species in the primary alumina in conjunction with the addition of primary alumina affected the emf immediately after addition, but the effect was reduced by the use of fully calcined alumina and a totally immersed probe.

Drifting in emf was observed in all experiments and might have several explanations. The reaction between dissolved metal, possibly stemming from the aluminium reference electrode, and CO and CO_2 is believed to be one of the main

reasons for the drifting. To get the aluminium leakage from the aluminium reference electrode under control and to develop a solid buffer system of CO and CO_2 seem important.

The use of graphite sensors for determination of alumina concentration in cryolite melts is not appropriate as long as other variations in the system influence the measured potentials. To get control of the other variables in the system will be important in the further development of this method of measuring the alumina concentration.

Sammendrag

Oppløsning av alumina er en av de mest avgjørende prosessene i produksjonen av primær aluminium med den såkalte Hall-Heroult prosess. Kartlegging av denne prosessen er en viktig faktor for å kunne forbedre elektrolyseprosessen for produksjon av aluminium. Å finne en metode for å måle aluminakonsentrasjonen i smelta er vesentlig for å forstå oppløsningsprosessen. Flere metoder har blitt testet i følge litteraturen. Målinger av elektromotorisk spenning er definert som differansen i spenning mellom en arbeidselektrode og en referanseelektrode, og er en metode som kan brukes til å studere oppløsning av alumina i kryolittsmelter. I denne masteroppgaven har målinger av elektromotorisk spenning i en elektrokjemisk celle bestående av en grafittsensor og to forskjellige referanseelektroder (en aluminiumreferanseelektrode og en grafittreferanseelektrode) blitt gjennomført for å finne ut om en grafittmaterialer er egnet for å bestemme aluminainnholdet i badet.

Resultatene viste en avtagende trend i spenning når alumina ble tilsatt smelten, men også at rett etter tilsats skjedde det en umiddelbar og voldsom endring i elektromotorisk spenning, enten i form av et hopp eller et dropp. Disse umiddelbare endringene er trolig grunnet andre endringer i systemet og ikke et resultat av en økende aluminakonsentrasjon. Systemets følsomhet for endring av andre variable har derfor blitt testet for å finne ut hvordan metoden kan utvikles til å gi troverdige aluminakonsentrasjonsmålinger.

En teori var at de umiddelbare endringene i spenning i forbindelse med tilsats av alumina kunne skyldes luft som aluminaen drar med seg ned til badet og der reagerer med karbon og danner CO og CO_2. En økning i partialtrykkene av CO og CO_2 vil føre til en økning i spenning. Også introduksjon av CO_2 til cella ga en økning i spenning og bygger derfor under at en økning i CO og CO_2 vil øke målt potensial. Hvis det er tilfelle at partialtrykkene av CO og CO_2 endrer seg, er antagelsen om konstant partialtrykk av CO og CO_2 gjort i de teoretisk beregningene av elektromotorisk spenning feil, og et solid buffersystem av CO og CO_2 vil være nødvendig for å hindre at CO og CO_2 påvirker målingene av elektromotorisk spenning.

Utvikling av gass i forbindelse med tilsats av primær alumina så ut til å gi en umiddelbar endring i målt spenning. Tilsats av kalsinert alumina og bruk av en grafittsensor som ikke er i kontakt med gassen over smelten ga derimot en mye

lavere umiddelbar endring av spenning ved tilsats.

Drifting i spenning ble oservert i alle eksperimentene. En av hovedgrunnene til driftingen kan være at metall fra aluminiumsreferansen som lekker ut i smelten i digelen og reagerer med CO og CO_2.

Bruk av en grafittsensor for å måle aluminakonsentrasjonen i kryolittsmelter er ikke egnet så lenge spenningen også varierer på grunn av andre endringer i smelten. Å få kontroll på andre variabler som påvirker potensialet må til for å kunne utvikle denne metoden å måle aluminakonsentrasjon på slik at den blir troverdig.

Table of Contents

List of Tables

List of Figures

Abbreviations and Symbols

Table 1: List of Abbreviations and Symbols.

Abbreviation/Symbol	Explanation
a_x	Activity of species x
BET	Braunauer, Emmett, Teller
CCD	Critical current density
D_{inner}	Inner diameter
D_{outer}	Other diameter
E	Cell potential [V]
emf	Electromotive Force
Exp.	Experiment
E^0	Standard cell potential [V]
F	Faraday's constant = 96485 C/mol
L.O.I	Loss on ignition
n	Number of moles of electrons per mole of products
P_x	Partial pressure of species x
PFC	Perfluorcarbon
T	Temperature (·C)
R	Gas constant = 8,314 J/(K·mol)

Chapter 1

Introduction

Aluminium is a very important metal since its properties benefit society in many ways. During the past few decades application areas for aluminium have steadily increased due to its many good properties. Aluminium has a natural protection against corrosion, it is a light metal compared with its mechanical strength, and it has good conductivity and it can be endlessly recycled without loss in quality. The automotive industry is one example of areas where alumina is about to replace traditional materials. The cars are getting lighter and are thereby using less fuel which contributes to lower emissions. Aluminium production makes up the largest part of the Norwegian metals industry and is one of Norway's largest export industries [1].

Aluminium is one of the most abundant elements in the earth's crust and it does not occur in nature as pure aluminium. Before the 19th-century alumina was a rare metal because it was difficult to synthesize large amounts of it. In 1886 Paul Héroult and Charles Hall independently of each other discovered and patented a process by which alumina or aluminium oxide, Al_2O_3, was dissolved in a electrolyte, mainly cryolite, and decomposed electrolytically to give aluminium. The Hall-Héroult process is named after its two inventors and is the only method by which aluminum is produced industrially today [2].

Alumina is one of the main raw material in primary aluminium production. To better understand the aluminium production process and to get a better process control, a better understanding of the raw material and its behaviour is important. This is becoming increasingly important as industrial pots become larger and with increased focus on emission of PFC gases and anode effect.

Alumina dissolution is one of the most important processes taking place in the Hall-Héroult process for the production of primary aluminium. The dissolution process is complex where several properties including the bath composition, bath flow conditions, bath temperature, alumina temperature, alumina properties and feeding method play an important role. The effective dissolution of alumina in the electrolyte is a decisive factor for the stable operation and design of aluminium reduction cells since undissolved alumina can forms muck, bottom sludge or crust which may give an increase in resistance and temperature and decrease in current efficiency. One of the key issues for advanced aluminium electrolysis is to identify and understand the dissolution mechanism and improve the dissolution process. [3]. To achieve reliable dissolution measurements is important in order to understand and improve the alumina dissolution process, and it will make it possible to compare different kinds of alumina and investigate the dissolution process under different conditions.

The main goal of this work is to be able to measure the alumina concentration in order to follow the dissolution process. There exist several potential methods for determining alumina concentration in the bath, either by sample taking followed by laboratory analysis or by in situ measurements. Electromotive force, emf, which is difference in potential between a working electrode and a reference electrode, is one way to study what happens when alumina is added to the cryolite melt. Because available electrodes usually have shown a low degree of reproducibility required for successful emf measurement there have only been done a few attempts in this field.

In this project, emf measurements are conducted between a graphite sensor and reference electrodes. The aim is to figure out if the graphite material is suited for determination of alumina concentration in cryolite melts. In order to achieve reliable alumina concentration measurements, it is important that changes in emf only are related to change in alumina concentration and not other variations in the system that impacts the measurements.

A suitable working electrode together with a reliable reference electrode might simplify the kinetic study when species are added to the melt and hopefully make it possible to achieve continuous measurements of the alumina concentration in the future. A stable reference electrode is crucial to the success of electrochemical measurements. The reference electrode is used for monitoring the potential when performing electrochemical experiments. Accurate emf measurements in molten cryolite have been difficult to achieve because it is hard to find reliable electrodes, container and diaphragm materials [4]. The problems related to the development of a reliable reference electrode for use in cryolite melts are due to the high temperatures and the corrosive environment which limits the choice of construction

materials and reference electrode reactions [5].

Grjotheim et al. [6] mention several reference electrodes used to study electrochemical equilibria and to derive thermodynamic data. Both gas electrodes, oxide electrodes, metal electrodes and electrodes with liquid junction have been designed. One of the reference electrodes highlighted is the aluminium reference electrode which has shown satisfactory stability and will be used in this project. The other reference electrode tested here is a self-designed graphite reference electrode.

Chapter 2

Theory

2.1 The Hall-Héroult Process

Today, nearly all aluminium is produced by the Hall-Héroult process. The Hall-Héroult process is an electrochemical process where alumina is dissolved in an electrolyte, mainly consisting of liquid cryolite, Na_3AlF_6, and is reduced to aluminium at about 960 °C. Carbon anodes are placed in the electrolyte and oxygen ions from dissolved alumina reacts with the carbon at the anode and forms carbon dioxide. Below the electrolyte in the cell there is a pool of liquid aluminium, where the interface between the metal pool and the electrolyte acts as the cathode. Aluminium is formed at this interface. The liquid aluminium is contained in preformed carbon lining inside a steel shell which is thermally insulated. Figure 2.1 shows a sketch of a modern Hall-Héroult cell [7].

The overall chemical reaction of the production of aluminium can be written as [7]:

$$2Al_2O_3(diss.) + 3C(s) = 4Al(l) + 3CO_2(g). \tag{2.1}$$

Some of the metal is dissolved in the electrolyte and may be reoxidized by the CO_2 gas produced at the anode according to the following reaction[8]:

$$2Al(diss.) + 3CO_2(g) = 2Al_2O_3(diss.) + 3CO(g). \tag{2.2}$$

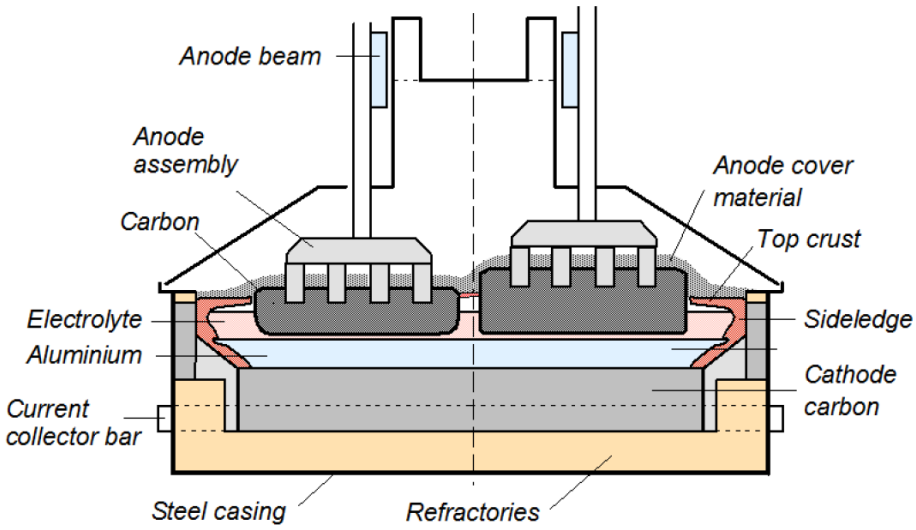

Figure 2.1: A sketch of a modern Hall-Héroult cell [9].

2.2 Cryolite Melts

The electrolyte used in the Hall-Héroult does mainly consist of cryolite. Cryolite is used due to its ability to dissolve aluminium oxide and for its high conductivity and stability. The melt consist of sodium fluoride, NaF, and aluminium fluoride, AlF_3, at the molar ration 1:3. Liquid cryolite consists of predominantly three anions: F^-, AlF_4^- and AlF_6^{3-} and one cationic species: Na^+. In melts saturated in Al_2O_3, there also exist several ions consisting of Al, O and F. Different kinds of additives are used in the electrolyte to change the chemical and physical properties of the melt in such a way so the current yield is increased $NaAlF_4$. The composition of the electrolyte changes during the electrolysis due to vaporization form the bath or reactions in the bath. The most important reaction that causes vaporization is formation of sodium fluoaluminate:

$$Na_3AlF_6(l) = NaAlF_4(g) + 2NaF(l) \tag{2.3}$$

Reactions between species in the bath are also changing the composition. The solubility of oxides in the melt is one reaction that may take place:

$$2Na_3AlF_6 + 3MeO = 3MeF_2 + 6NaF + Al_2O_3 \tag{2.4}$$

An other reaction that contributes to change in the bath composition is reaction with moisture:

$$2Na_3AlF_6 + 3H_2O = Al_2O_3 + 6NaF + 6HF \tag{2.5}$$

An electrolyte that has a surplus of AlF_3, a molar ratio of NaF to AlF_3 that is less than 3, is defined as an acidic electrolyte. An acidic melt is preferable in aluminium electrolysis since it makes it possible to run the cell at a lower temperature which is positive for the production. AlF_3 is added to the bath to maintain the bath acidity [2] [10].

2.3 Alumina Production and Properties

Alumina is the raw material in the Hall-Héroult process. It is manufactured from bauxite through the Bayer process. The Bayer process is described in section 2.3.1. Theoretically, 1.89 kg Al_2O_3 gives 1 kg Al. On time average the electrolysis cell has an alumina concentration of 2 to 4 mass%. A too low concentration may lead to an anode effect. During anode effect, the normal reactions that produce aluminium are interrupted and fluoride components of the bath are decomposed electrolytically. Gases, CO, CF_4 and C_2F_6, are formed and create an electrically insulating gas layer underneath the anode, which is the reason for why the voltage of the cell increases to very high cell voltages. It is also important that the alumina dissolves and mixes rapidly in the bath after addition and that it does not form any sludge. Sludge is mainly undissolved bath and alumina slurry which ends up beneath the metal pad.

In order to replenish the electrolyte properly, the alumina needs to meet certain criteria [2]:

1. A sufficient quantity of alumina needs to be delivered to the liquid bath.
2. The alumina need to be dispersed in the feeding zone and dissolved rapidly within the electrolyte.
3. To avoid anode effects a minimum concentration of alumina is needed under each anode, which means that it needs to be sufficiently distributed.

Today there exist strict specifications for the alumina used in the aluminium production. The quality of the alumina is important for both the cell operation and the

metal purity. Only small variations in the Bayer process may give significant differences in the physical and chemical properties of the material. Different alumina producers may therefore produce a product of varying quality.

Historically, alumina has been divided into two categories: ”sandy” and ”floury”. The sandy one has been calcined at a lower temperature and has coarser crystals with higher BET surface area. It has a low content of fines and low content of the alpha phase. The floury alumina has been calcined at higher temperatures and contains more alpha phase. It has a high content of fines and is dustier and has a low BET surface area.

Alumina is also used in the cleaning process of exhaust gas from the cell. The oxide absorbs the fluorides and other pollutants and is thereby used in the aluminium production. By using alumina in this way the loss of fluoride is reduced and some of the undesirable pollutants are accumulated. The oxide is denoted primary oxide before it is used in the scrubbers and secondary oxide when it exits the scrubbers.

The third major role of alumina in the process is as anode cover material. Alumina together with frozen bath makes a thermally insulation crust which contributes to reduce heat loss from the cell in addition to avoid air burn and hindering emissions through the top of the cell [2].

2.3.1 The Bayer Process

The Bayer process is the principal industrial means of refining bauxite to produce alumina. It was developed and patented in 1888 by Karl Josef Bayer. Bauxite contains 40-60$\%$ of alumina and is the most important ore for the production of alumina. Since 1888 has the Bayer process been the dominating process for alumina production for the aluminium industry with an annual production of about 37 million tonnes [8].

The first step in the process is extraction where the hydrated alumina is extracted from the insoluble components in a solution of sodium hydroxide. The insoluble components are mostly oxides, such as silica, iron oxides and titanium dioxide. Rapid dissolution of the oxide requires the ore to be in a fine particle size, a certain concentration of sodium hydroxide and a certain temperature and pressure. To achieve the fine particles, the ore is crushed and milled, which makes the minerals more amenable to extraction. The sodium hydroxide concentration, the operating pressure and the operating temperature varies with the nature of the bauxite ore.[8]. Ores that contain much of the aluminium-bearing mineral gibbsite can be processed at 140 °C with about $110 \mathrm{gl}^{-1}$ of Na_2O, while processing of Böhmite re-

quires harsher conditions, between 200 °C and 240 °C and 140-170gl^{-1} of Na_2O. The pressure is defined by the steam pressure during the actual process conditions and is for instance 35 atm for 240 °C [11].

The extraction can be described by the following equation

$$2Al_2O_3 \cdot xH_2O + NaOH \rightarrow 2NaAlO_2 + (x+1)H_2O \tag{2.6}$$

.

After the extraction the solution is fed through a slowly agitated settling tank, where the coarse insoluble material settles out. To remove most of the silica that has dissolved in the solution, the liquor is diluted and mixed with more insoluble material to allow precipitation of an insoluble sodium aluminium silicate. Then the solution is separated from the mud in tray thickeners. This process is often aided by a coagulating material such as starch. In the very end of this stage of the process, the liquor is filtrated before it goes to the second step in the process [10].

The next part of the process is the decomposition, where crystalline aluminium trihydrocide is precipitated from the liquor. The precipitation can be described by the following equation

$$2NaAlO_2 + 4H_2O \rightarrow Al_2O_3 \cdot 3H_2O + 2NaOH, \tag{2.7}$$

and is basically the reverse of the extraction reaction. In this reaction it is desirable with cooling, dilution and as the precipitated alumina hydrate usually is gelatinous seed crystals need to be added to control the structure of the precipitate. The decomposition is a very slow process and the rate increase with increasing crystal surface area, so excess amounts of crystalline seed must therefore be added. The decomposition is usually carried out at 50 °C for 25-30 hours. When the reaction reaches a very slow rate, the decomposition is stopped and the alumina trihydrate crystals are washed, the third step of the process can take place [10].

The third step is calcination of aluminium trihydroxide to form alumina that is suitable for the aluminium production, equation 2.8. The calcination process can be varied to lead to products that have different crystalline forms. Both heating rate and the particle size of the α-alumina hydrate plays a role when it comes to what product which is made. Figure 2.2 illustrates three different paths that have been reported for the conversion to α-alumina [10].

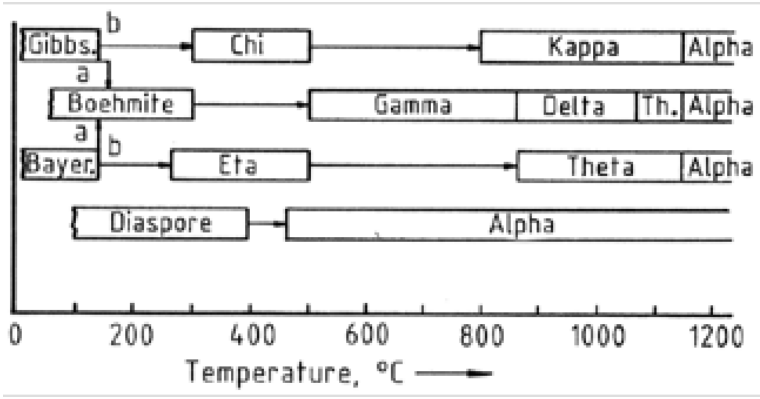

Figure 2.2: Three basic paths for dehydration of α-alumina trihydrates in air. Slow heating in path a, fast heating in path b and fine particles in path c [12].

In the first step of the calcination, at temperatures between 400 °C and 600 °C, most of the water of the crystallization is removed and alumina in the active gamma phase is formed. When it is heated further, the γ-alumina is converted to α-alumina which is more inert [8]. Since the calcination mechanism is complex the residual water content, surface area and density of the alumina will be dependent on the final heating temperature[10].

$$Al_2O_3 \cdot 3H_2O \rightarrow Al_2O_3 + 3H_2O \tag{2.8}$$

2.3.2 Properties of smelter grade alumina

Grjotheim et al. [2] presents several properties, both chemically and physically, which are used to characterize alumina. In this section the most important ones will be presented. Not all of the presented properties are relevant in this thesis, but may be relevant in further work.

Chemical Purity

Alumina contains impurity oxides and the content of these oxides are important for the metal quality and the cell performance. The most important impurities are sodium oxide and calcium oxide, while silica, titania, iron oxide and the oxides of phosphorous and vanadium represent minor impurities. Most aluminas have a sodium oxide content of 0.5 to 0.6 mass%. Sodium oxide reacts with AlF_3 in the bath and forms cryolite. Calium oxide is present in much lower contents, but is important since it is the major source for the CaF_2 in the bath [2].

Alpha Alumina (α-Al_2O_3)

Alpha phase and gamma phase are the main phases of alumina in the electrolysis cell. A typical alpha content is between 5 and 80 mass%, but 10 to 30 wt% are most common for the aluminas used today. The alpha content is of importance since it is connected with the crust formation and it hardness, density and thermal conductivity. An alpha phase content below 30 mass% is needed to get a stable crust and even lower values are needed to obtain the best crust quality [2].

BET Surface Area

The BET surface area, Braunauer, Emmett, Teller surface area, is a technique where the physisorption of nitrogen is used to to calculate the surface area of a particle. The BET surface area varies from 5 m^2/g for floury aluminas to 100 m^2/g for sandy aluminas. The surface area is important for the rate of dissolution in the bath, a higher BET surface area gives a greater dissolution rate [13]. It is also an important property for the alumina used in the scrubbers to ensure sufficient absorption of gas [2].

Attrition Index

The strength of the agglomerated grains to resist mechanical handling and transport without being crushed into finer particles [2].

Density

Two different densities are used to describe alumina; bulk and real density. The real density is measured after alumina has been finely ground and is determined by filling the void fractions in the alumina with a volume. The bulk density is usually found by filling alumina in a vertical cylinder and measuring its volume. The bulk density is a property of great interest because the alumina feeders inn the cells measure the alumina dumps by volume, so it may cause inconsistencies in the mass of alumina added to the cell and thereafter also the consentration of alumina in the cell and thereby on the cell operation. The bulk density is also important for the quality and properties of the crust [2].

L.O.I.

Loss On Ignition, L.O.I., is the mass loss of humidity or moisture of the alumina when it is heated between specified temperatures in an inert atmosphere. For aluminium smelters heating between 300 °C and 1000 °C is most often chosen since it also give an indication on if the calcination to decompose the hydrates in the Bayer process has been effective. L.O.I. is a very important property in characterization of alumina. It is indirectly related to several other properties (alpha content, BET surface area, bulk density and degree of calcination of the alumina) [2].

Alumina with L.O.I. values between 0.5 % and 0.9 % are most often required, since high water content may cause increased fluoride emissions thorough hydrolysis [2].

Particle Size Distribution

The particle size of alumina is preferred to be between 20 and 150 μm. Too big particles is unwanted because they have low rate of solution in the bath, while very small particles, fines, is harmful due to dust emission and mechanical handling problems [2].

Porosity

Porosity is not the most important measure of the quality of aluminas, but it can be related to the real density and the alpha content in the alumina. The porosity can be measured by absorption of water or carbon tetrachloride, and then a porosity index can be determined [2].

2.4 Alumina Dissolution

The dissolution of alumina in cryolite melt consists of several steps between the discharge of alumina powder from the addition to the formation of a homogeneous solution in the electrolyte. These steps include: to heat up alumina sufficiently, the transformation of gamma-alumina to alpha-alumina, dissolution of alpha-alumina and chemical reaction with ions to form aluminium oxyfluoride species and mixing of the dissolved solution to get a uniform electrolyte. Several factors can strongly

influence the dissolution process. Such factors can be chemical reactions or physical processes such as clump formation and dispersion. In the dissolution process, both heat transfer and mass transfer can be rate determining [2].

The dissolution process can be divided into four steps when assuming alumina of the sandy type and that the alumina is cold relative to the bath when being added [14].

1. The alumina hits the bath surface and it spreads on the surface. Then bath will freeze around the particles that are in direct contact with the bath. A frozen crust is formed for a short while, then heating occurs and remelting and further wetting take place. If there is not enough heat available a permanent crust will be formed.

2. Transition from gamma-alumina to alpha-alumina. At the same time, alumina particles will start sintering together.

3. Before further dissolution can occur the frozen electrolyte need to melt. When the frozen bath has melted away the alumina grains are partly sintered together and tend to form large agglomerates or lumps which might sink in the melt.

4. The dissolution process starts as soon as the alumina is exposed to the bath. This process involves strong interaction with the fluoride melt while oxyfluoride species are formed. The overall dissolution rate is dependent on the exposed surface area. This area can vary within several orders of magnitude depending on whether lumps have been formed or whether individual alumina particles are dispersed in the melt.

Step 1 in the process is obviously heat transfer controlled since the process involves freezing and melting of bath around the alumina grains. Step 2 is harder to describe from the theory, but is believed to be dependent on the composition of the added alumina. For step 4 there exist three different possibilities that can be rate determining; heat transfer, mass transfer and slow chemical reactions.

Even though the structure of the cryolite-alumina melts is a widely investigated subject, it is still not completely resolved. Several suggestions regarding possible structural species in the cryolite-alumina melts have been made, but it is now generally agreed that aluminium-oxygen-fluoride [2].

According to several studies mentioned by Thonstad et al. [7] $Al_2OF_6^{2-}$, $Al_2OF_8^{4-}$ and $Al_2O_2F_4^{2-}$ are the most important oxygen containing ionic entities at low alumina concentrations, and these species may be formed by the following reactions [2]:

$$4AlF_6^{3-} + Al_2O_3 = 3Al_2OF_8^{4-} \tag{2.9}$$

$$4AlF_6^{3-} + Al_2O_3 = 3Al_2OF_6^{2-} + 6F^- \tag{2.10}$$

$$AlF_6^{3-} + Al_2O_3 = 1.5Al_2O_2F_4^{2-} \tag{2.11}$$

At higher alumina consentration $Al_2O_2F_4^{2-}$ and $Al_2O_2F_6^{4-}$. The latter species also requires F^- ions as reactants [2]:

$$3F^- + AlF_6^{3-} + Al_2O_3 = 1.5Al_2O_2F_6^{4-}. \tag{2.12}$$

Cell operational problems may happen if the alumina is not dissolving efficiency, therefore the rate of dissolution of alumina is of great importance. Unluckily, the rate of dissolution is not only dependent on the bath conditions, but the way the alumina is added and the physical and chemical characteristics of alumina powder are decisive factors [2]. The physiochemical properties of alumina related to the dissolution rate of alumina include commonly specified and measurable parameters: density, surface area, alpha phase content, particle size distribution, water content, attrition index and chemical composition [13].

Reliable laboratory measurements of alumina dissolution rates are very hard to achieve due to the three ways alumina can dissolve [2]:

1. It rapidly disperses as discrete grains and dissolves easily.
2. It may sink without dispersing.
3. It may form clumps due to agglomerate of alumina and frozen bath around it. This clumps may float on the electrolyte surface or sink to the bottom of the cell.

The cell conditions giving the worst dissolution rate would be a bath with high alumina concentration, high acidity and low superheat and low velocity. The cell operational variables are very important for the rate of dissolution and may give as much as a thirty-fold increase in the dissolution rate. The alumina quality is also an important variable, but can only cause a doubling of the rate[2].

It has been sown that the concentration of alumina in the bath affect the rate of the dissolution. According to Gjortheim et al. [8] several authors reports that an increasing content of alumina up to 10 wt$\%$ decreases the rate of dissolution steadily.

2.5 Cell Reactions and Theoretical Cell Potentials

The cell reactions between a graphite sensor and the two different reference electrodes used in the experiments have been derived together with the corresponding Nernst equations. Estimation of theoretical emf values for the cells are also done. The graphite sensor can be either a graphite electrode or the carbon crucible.

Graphite Sensor versus Graphite Reference Electrode

Consider an crucible with bath in which a graphite electrode is immersed as seen in Figure 2.3. A second graphite electrode is placed inside a boron nitride tube, which is also immersed in the bath. A small hole in the boron nitride tube ensures contact between the bath inside the tube and in the crucible. The bath inside the tube is saturated with alumina. The graphite electrode in the boron nitride tube serves as the reference electrode. Two chambers are defined in the cell in order to derive the cell reactions and Nernst equation for the cell reaction. Chamber I is defined as graphite reference electrode and chamber II is defined as the bath in the crucible which surrounding the reference electrode.

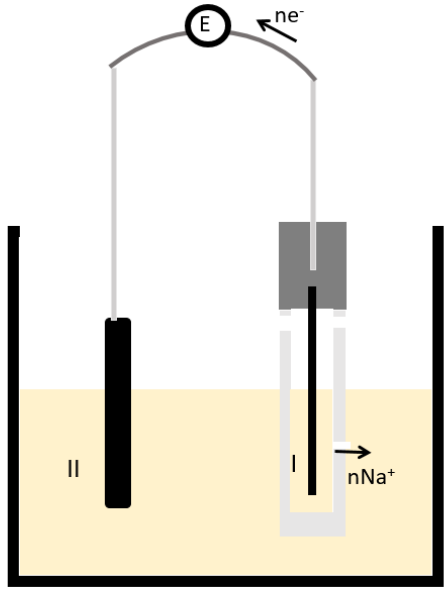

Figure 2.3: Illustration of a cell where the emf is measured for a cell consisting of a graphite sensor and a graphite reference electrode.

In chamber I oxide reacts with carbon as in equation (2.13). The oxide is given as O^{2-} in the equation, but in reality, other oxide compounds may be present as well. The chemical compounds are labelled with a roman number indicating in which chamber it is located. The electrochemical reaction which takes place in chamber II is shown in equation (2.14). Equation (2.15) represents the migration of sodium ions from chamber I to chamber II in order to maintain the charge neutrality. To keep it simple sodium ions are assumed to be the only charge carrier since it is believed to be the most important charge carrier, but in reality other ions such as fluoride may be charge carriers as well.

$$I \qquad O_I^{2-} + C_I = 2e^- + CO_I \qquad (2.13)$$

$$II \qquad CO_{II} + 2e^- = C_{II} + O_{II}^{2-} \qquad (2.14)$$

$$III \qquad Na_I^+ = Na_{II}^+ \qquad (2.15)$$

$$I + II + 2III \qquad \begin{aligned} &C_I + CO_{II} + Na_2O_I \\ &= CO_I + C_{II} + Na_2O_{II}, \\ &E^0 = 0\,V \end{aligned} \qquad (2.16)$$

Nernst equation for the reaction is given in equation (2.17), where n is equal to 2.

$$E = \frac{-RT}{nF} \cdot ln \frac{P_{CO_I} \cdot a_{Na_2O_{II}} \cdot a_{C_{II}}}{P_{CO_{II}} \cdot a_{Na_2O_I} \cdot a_{C_I}} \qquad (2.17)$$

The activity of CO in the expression above is expressed as the partial pressure of CO above the melt since the absorbed amount of CO absorbed on the electrode is believed to be in equilibrium with the amount of CO in the melt and CO present in the gas above the melt. Since the temperature is high these equilibrium reactions are believed to be achieved very fast.

The expression in equation (2.17) can be simplified to equation (2.18) if a_{C_I} is equal to $a_{C_{II}}$, which is true if the same sort of carbon is used in the both of the electrodes, and if the carbon monoxide pressures is constant and the same in camber I and II. A constant partial pressure of CO is not necessarily true since airburn, reaction between oxygen and the crucible and carbon electrodes, may take place due to oxygen in the nitrogen gas (purity: 5.0) and introduction of air in conjunction

with the addition of alumina or other adjustments of the furnace setup. The formation of CO_2 and CO in the melt due to the reaction between alumina and carbon is believed to be absent, since no current is added. The case would be different in an industrial cell due to continuous CO_2 and CO production at the anodes.

$$E = \frac{-RT}{2F} \cdot ln \frac{a_{Na_2O_{II}}}{a_{Na_2O_I}} \tag{2.18}$$

By using data from FactSage, see Figure A.1 in Appendix, it can be found that the Na_2O activity versus the alumina concentration is is roughly linearly related, which gives another simplification of the Nernst equation, equation (2.19), since the activity coefficient of Na_2O is approximately equal to constant.

$$E = \frac{-RT}{2F} \cdot ln \frac{wt\%Al_2O_{3II}}{wt\%Al_2O_{3I}} \tag{2.19}$$

The cell reactions can also be derived by basing the cell reactions on CO_2 instead of CO since they are in equilibrium and will lead to the same expression for the potential. By assuming CO_2 in the cell instead of CO the following reaction will take place. The reaction in equation (2.20) takes place inside the reference, the reaction in equation (2.21) takes place in chamber II and the reaction in equation (2.23) represents migration of sodium ions from chamber I to chamber II.

$$I \qquad 2O_I^{2-} + C_I = 4e^- + CO_{2_I} \tag{2.20}$$

$$II \qquad CO_{2_{II}} + 4e^- = C_{II} + 2O_{II}^{2-} \tag{2.21}$$

$$III \qquad Na_I^+ = Na_{II}^+ \tag{2.22}$$

$$I + II + 4III \qquad \begin{aligned} &C_I + CO_{2II} + 2Na_2O_I \\ &= CO_{2I} + C_{II} + 2Na_2O_{II}, \\ &E^0 = 0V \end{aligned} \tag{2.23}$$

Nernst equation for the reaction is given in equation (2.24), where n is equal to 4.

$$E = \frac{-RT}{nF} \cdot ln \frac{P_{CO_{2_I}} \cdot a_{Na_2O_{II}}^2 \cdot a_{C_{II}}}{P_{CO_{2_{II}}} \cdot a_{Na_2O_I}^2 \cdot a_{C_I}} \tag{2.24}$$

The expression can be simplified to the same as in equation (2.19) if the same sort of carbon is used in both of the electrodes and if it can be assumed that the pressure of carbon dioxide is constant in both chambers.

It can be seen from equation (2.19) that the cell potential is a function of temperature and concentration of alumina in chamber II since the concentration of alumina in chamber I is supposed to be constant. Figure 2.4 shows how the potential varies with variation in temperature at different alumina concentrations. The variation in temperature has less impact at higher alumina concentrations. The cell potential is a logarithmic function of the alumina concentration, Figure 2.5, and greater variations will be seen in the first additions of alumina, while when the concentration in chamber II is getting closer to saturation the effects on the cell potential gets smaller and smaller.

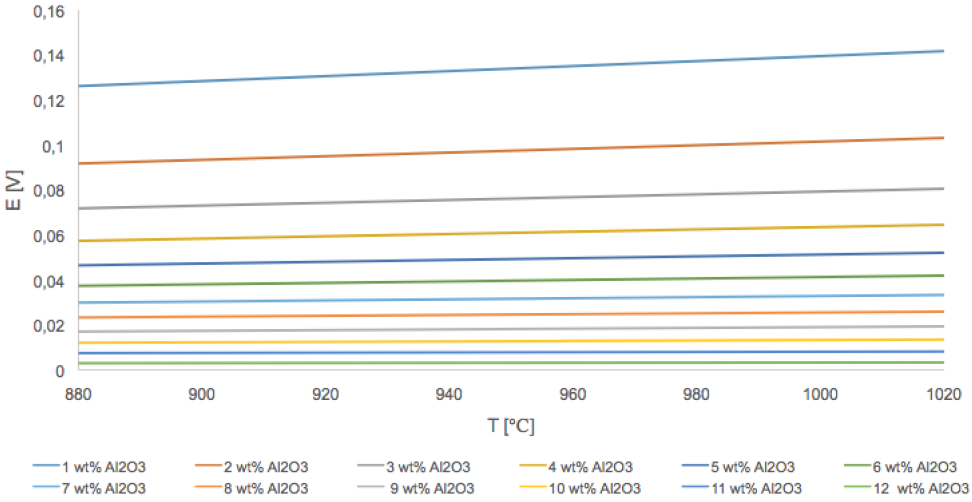

Figure 2.4: Theoretical values of the potential between a graphite sensor and a graphite reference electrode as a function of temperature at different alumina concentrations. The calculations are based on equation (2.19).

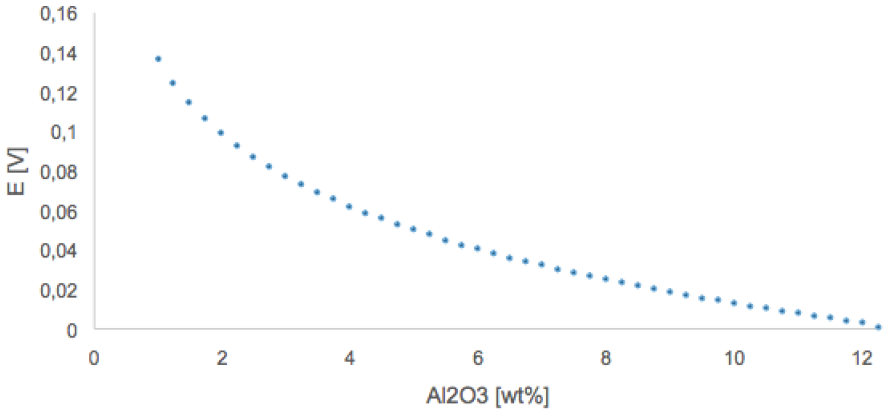

Figure 2.5: Theoretical values of the potential between a carbon electrode and a graphite reference electrode as a function of alumina concentration. Equation (2.19) is used in the calculations and the temperature is set to 970 °C.

Graphite Sensor versus Aluminium Reference Electrode

A cell consisting of a graphite sensor and an aluminium reference electrode is shown in Figure 2.6.

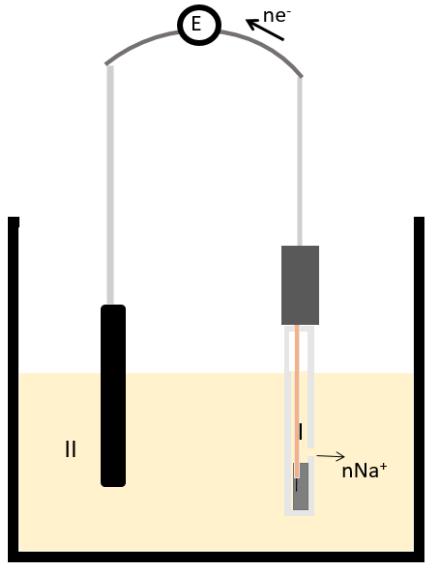

Figure 2.6: Illustration of a cell consisting of a graphite sensor and an aluminium reference electrode.

The aluminium reference electrode used in this project was designed as will be described in Chapter 4. The graphite crucible or a graphite electrode was acting as the graphite sensor. The aluminium reference electrode is denoted as chamber I and the bath in the crucible is defined as chamber II. The reactions taking place in the compartment are shown in equation (2.25), (2.26) (2.27), (2.28) and (2.29) and the Nernst equation for the cell is given in (2.30)

$$I \qquad Al_I = 3e^- + Al_I^{3+} \qquad (2.25)$$

$$II \qquad CO_{II} + 2e^- = C_{II} + O_{II}^{2-} \qquad (2.26)$$

$$III \qquad Na_I^+ = Na_{II}^+ \qquad (2.27)$$

$$IV \qquad O_I^{2-} = O_I^{2-} \qquad (2.28)$$

$$2I + 3II + 6III + 3IV \qquad \begin{aligned} &2Al_I + 3CO_{II} + 3Na_2O_I = \\ &Al_2O_{3I} + 3C_{II} + 3Na_2O_{II} \\ &E^0(T) \neq 0\,V \end{aligned} \qquad (2.29)$$

$$E = E^0(T) - \frac{RT}{6F} ln \frac{a_{Al_2O_{3I}} \cdot a_{C_{II}}^3 \cdot a_{Na_2O_{II}}^3}{a_{Al}^2 \cdot P_{CO_{II}}^3 \cdot a_{Na_2O_I}^3} \qquad (2.30)$$

The Nernst equation can be simplified to equation (2.31) by assuming that the activity of carbon and aluminium are equal to 1.

$$E = E^0(T) - \frac{RT}{6F} ln \frac{a_{Al_2O_{3I}}}{P_{CO_{II}}^3} - \frac{RT}{2F} ln \frac{a_{Na_2O_{II}}}{a_{Na_2O_I}} \qquad (2.31)$$

At saturation, the activity of alumina is 1 so $a_{Al_2O_{3I}}$ is assumed to be 1 in equation (2.31). The Na_2O activity versus the alumina concentration is is roughly linearly related, so the activity of Na_2O can be replaced with the alumina concentration since the ratio of the Na_2O activities in chamber II and I will be the same as the ratio of the alumina concentrations in chamber II and I. Equation (2.31) can therefore be simplified to equation (2.32). The partial pressure of CO is unknown, but can be estimated by assuming a cell potential of 1 V at an alumina concentration of 1 wt% since in most of the experiments the potential started somewhere

around 1 V when the concentration was $\sim$1 wt%. $E^0(T)$ can be found from FactSage and are listed for some temperatures in Table B.1 in Appendix B. 970 °C is used in the calculations since the temperature in the melt usually was approximately 970 °C. By rearranging the equation below and insert the values mentioned above a partial pressure of CO equal to 0.022 atm can be found.

$$E = E^0(T) - \frac{RT}{6F} ln \frac{1}{P^3_{CO_{II}}} - \frac{RT}{2F} ln(\frac{wt\%Al_2O_{3II}}{wt\%Al_2O_{3I}}) \tag{2.32}$$

Figure 2.7 shows how the potential will change when assuming constant activity of Al_2O_3 and Na_2O in chamber I and a constant pressure of CO equal to 0.022 atm. The assumption of constant partial pressure of CO may not be correct as discussed in section 2.5 and the calculated values for the potential may deviate from what is reality, but Figure 2.7 gives an indication of how the potential may change during an increasing alumina concentration.

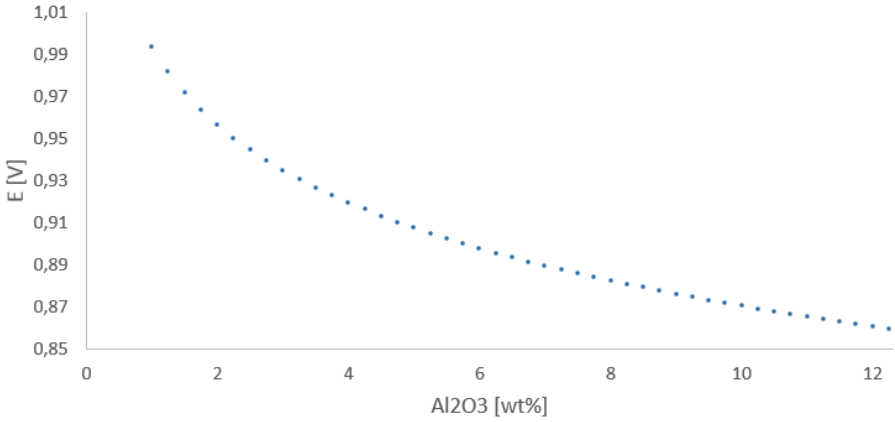

Figure 2.7: Calculated values of the potential between a carbon electrode and a aluminium reference electrode as a function of alumina concentration. The calculations are based on equation (2.32).

Chapter 3

Previous Work within the Field

3.1 Studies of Alumina Dissolution

Several methods have been used in former studies for monitoring the alumina dissolution. From available literature, it becomes apparent that most of the research has been conducted using laboratory experiments. This chapter will discuss some of the previous work done in this field.

Haverkamp et al. [15] mention several methods that have been used for studying alumina dissolution. Early methods were based on visual observations of the alumina grains. Dissolution was considered to have taken place when no grains were visible in the melt. These methods were not very accurate since the similar refractive index of the melt and the alumina particles made it difficult to determine when the dispersed alumina had dissolved completely. The most successful methods and where most effort has been directed are according to Haverkamp et al. electrochemical techniques. The methods reported are chronopotentiometry, sweep voltammetry and electrochemical method based on impedance.

Chronopotentiometry is one of the methods that has been used. The aim is to find a critical current density for which anode effect occurs. The reproducibility of this method is reported to suffer from poisoning of the carbon electrode by the perfluorocarbon, PFC, during anode effect. Sweep voltammetry gave inaccurate measurements due to the slowness of the method which caused large consumption of the carbon electrode. The electrochemical method based on impedance was too slow to measure the rapid alumina dissolution. Haverkamp et al. developed a method based on a modified linear sweep voltammetry, and this method has

been used with success to study dissolution behaviour of aluminas at conditions that are similar to cell operating conditions. Haverkamp's method differs from conventional linear sweep voltammetry since the forward sweep rate is fast and continues until anode effect, 30 V/s, and the reverse is very fast, 300 V/s. The occurrence of the anode effect is fundamental to the procedure. Since the sweep rates are fast the problem associated with anode consumption is low and evolution of gas becomes minimal [15].

Richard et al. [16] have done a review of publications in the alumina dissolution field. The fast linear sweep voltammetry, often termed as critical current density (CCD) in this context, seem to be the most promising method of in situ alumina concentration determination. The actual dissolved alumina content is determined using a precalibrated apparatus and an electrochemical probe. According to Richards et al. the concerns with the method is the design and use of the probe. The concerns are the reproducibility in different hydrodynamic conditions, reproducible calibration curves modes of applied current or voltage, influence of electrode shape and influence of CO/CO_2 bubbles on the surface.

Vasyunina et al. [17] studied the solubility and dissolution rate of alumina in acidic cryolite aluminous melts by the use of an electrochemical method based on a measurement of the equilibrium electromotive force (emf). The cell investigated was Pt, O_2 | $Al_2O_{3(sat)}$, Na_3AlF_6, AlF_3 | Na_3AlF_6, AlF_3, $Al_2O_{3(notsat)}$ |O_2, Pt when portions of alumina were added. A sketch of the cell is shown in Figure 3.1 and Figure 3.2 shows an example of the emf response.

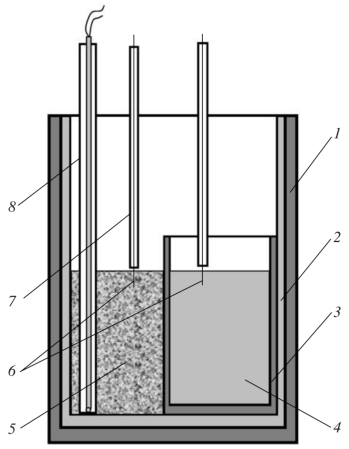

Figure 3.1: The experimental setup used by Vasyunina et al. 1-graphite crucible, 2-aluminium crucible, 3-internal graphite crucible, 4-electrolyte, 5-electrolyte saturated with alumina, 6-platinum electrodes, 7-corundum tubes and 8-thermocouple.[17].

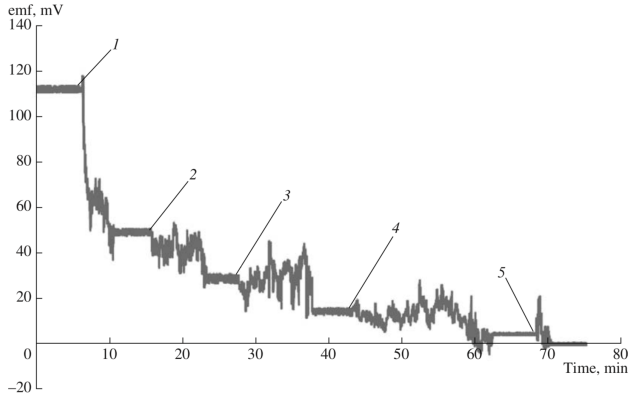

Figure 3.2: Results from Vasyunina et al. Emf values as a function of time. 1–5 correspond to loadings of alumina from first to fifth [17].

3.2 Aluminium Reference Electrode

Aluminium reference electrodes of different kinds have been used in several studies and shown satisfactory stability as a reference electrode. Drossbach introduced the aluminium electrode in 1936 and it has later been adopted in a number of studies. The reference electrode does usually consist of an aluminium electrode placed inside a tube of boron nitride or sintered alumina. The contact wire can be tungsten, tantalum or molybdenum and a small hole in the tube connects the electrode to the bulk cryolite electrolyte. There has been reported small drifts or fluctuations in the potential which may be due to complications with the contact wire as some of the metal has a tendency to dissolve in aluminium to form intermetallic compounds. Variations in the composition of the melt close to the electrode or dissolving of metal into the melt can also affect how the aluminium electrode behaves [6].

Bergman et al. [5] used a variant of aluminium reference electrode where aluminium and a mix of cryolite and alumina were placed inside a closed alumina tube. The contact wire was of molybdenum, where only the tip was wetted with liquid aluminium, while the rest was protected by an alumina tube. The measured potential between two such reference electrodes was found to be stable within 5 mV for more than 8 hours [7].

Sadoway [18] designed and used another variant of an aluminium reference electrode where the aluminium pool floated on top of the melt inside the reference.

This was done to avoid contact between the electrolyte and connection wire. It was done by altering the density of either the electrolyte or the aluminium.

Sterten et al. [4] studied the behaviour of oxygen and aluminium electrodes by emf measurements in cryolite melts saturated with alpha-alumina. They described the aluminium reference electrode as reversible, but that it reacts to some extent with the electrolyte resulting in a reduced NaF activity and an increased AlF_3 activity.

Aluminium reference electrodes have also been used in industrial cells where they have shown successful. Some designs have shown a durability of several days [7].

Chapter 4

Experimental

This section describes the experimental work done in this master thesis. Design of reference electrodes, design of a laboratory cell, testing of the electrodes and measurements of the emf while alumina is added have been done.

4.1 Design of Electrodes

Two different graphite electrodes and two different reference electrodes have been designed and used in these experiments. The graphite reference is self-designed while the aluminium reference is inspired by the one used by Sommerseth [9].

4.1.1 The Graphite Reference Electrode

The graphite reference electrode designed for this project is shown in Figure 4.1a. A carbon rod (5 mm) was mounted to graphite connector and placed inside a boron nitride tube (D_{inner} = 10 mm, D_{outer} = 22 mm). A hole (1.5 mm) was drilled 3 cm above the bottom of the tube and two holes were drilled approximately 6 cm above the bottom of the tube to let gas get out of the tube. A steel rod connector bar (50 cm) was mounted to the graphite connector. Approximately 3 g of alumina was added to the tube in order to make a saturated solution in the tube. The reference electrode was heated gradually before it was placed in the electrolyte in order to not damage the boron nitride tube.

4.1.2 The Aluminium Reference Electrode

The aluminium reference electrode is commonly used in laboratory scale and various designs are described elsewhere [19, 5, 9]. A sketch of the reference electrode used in this thesis is shown in Figure 4.1b and is primarily based on the reference electrode described by Sommerseth [9]. The reference electrode was made of a boron nitride tube (D_{inner} = 5 mm, D_{outer} = 10 mm) connected to a steel tube. Approximately 0.65 g of aluminium was placed inside the boron nitride tube, and a hole (1.5 mm) which allowed for electrolyte penetration was drilled 3 cm above the outer bottom of the tube. A tungsten wire was threaded through an alsint (aluminium oxide) tube and placed inside the steel tube. 10 mm of the tungsten wire was left uncovered by the alsint tube. The alsint tube and the tungsten wire were lowered into the boron nitrid tube when the aluminium had melted. It was important to be careful when lowering the tungsten wire in order to make sure the wire did not slip inside the alsint tube and to make sure that the boron nitrid did not get damaged. When the reference electrode was placed in the furnace it was lowered to the bottom of the crucible and lifted 1 cm above the bottom. The reference electrode was then left in the cell for at least one hour to let electrolyte enter and let the system settle.

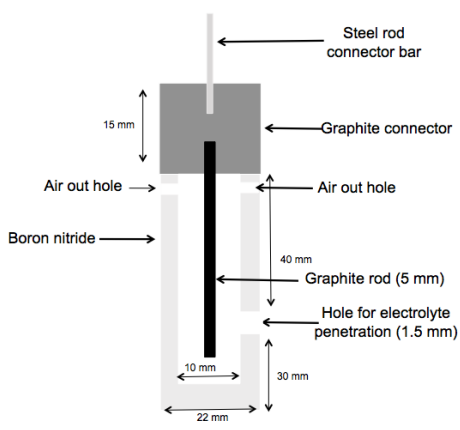

(a) The graphite reference electrode.

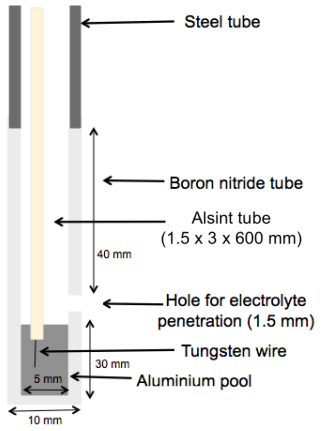

(b) The aluminium reference electrode.

4.1.3 Graphite electrodes

The graphite sensors used were both the crucible and graphite electrodes. When the crucible was used as sensor the voltage was measured at the crucible holder (a

steel rod) The graphite electrodes are shown in Figure 4.2a and 4.2b. The electrode illustrated in Figure 4.2a is a plain graphite electrode and the electrode shown in Figure 4.2b is a electrode where the graphite part is not in contact with the gas phase above the melt, referred to as the totally immersed electrode. The graphite electrodes were made in the same type of graphite as the graphite rod used in the graphite reference electrode. The crucible which also acted as a graphite sensor is not guaranteed to be made of the same type of carbon as the graphite reference.

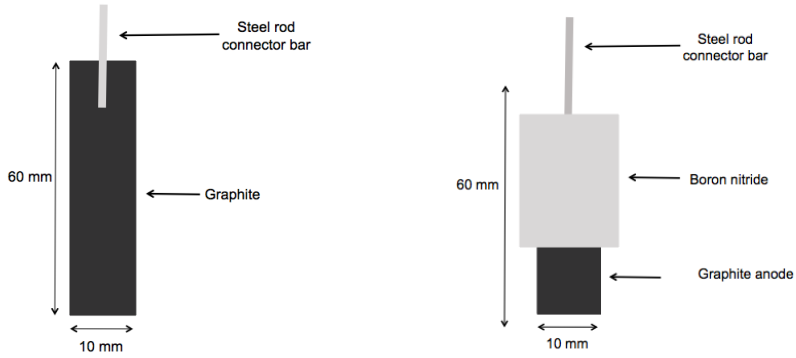

(a) The graphite electrode. **(b)** The totally immersed graphite electrode.

Figure 4.3 shows how the graphite reference electrode looked before it was inserted to the furnace and how the inside of the graphite reference electrode and the aluminium reference electrode looked like after use.

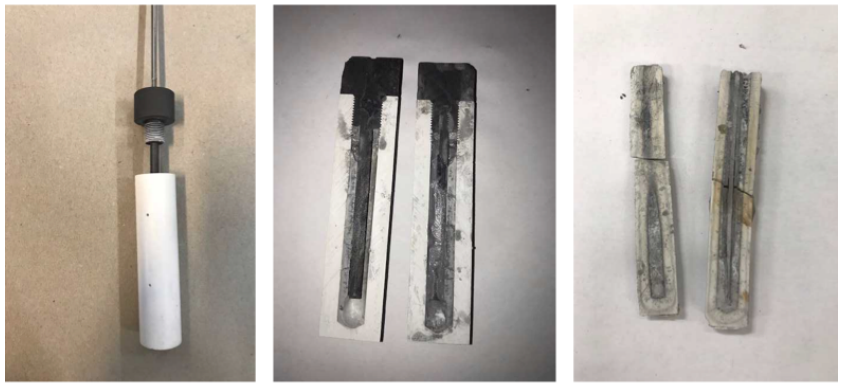

Figure 4.3: Pictures of the reference electrodes. From the left: Graphite reference, spent graphite reference, spent aluminium reference.

4.2 Apparatus Setup

Figure 4.4 shows the setup of the apparatus. It consisted of a water cooled cylindrical furnace equipped with an adjustable crucible holder in the bottom for elevate and lowering the crucible containing the electrolyte. The furnace was heated by a power supply and can reach a operating temperature of 1050 °C. A logger (Keithley 2000 multimeter) was connected to the electrodes and the thermocouple and used to measure the voltage and the temperature. Nitrogen gas was flowed through the furnace and exited through the top lid.

All electrodes, the feeding tube and the thermocouple were fastened by plugs to the top lid and silicone was used to seal to prevent gas leak. The temperature in the furnace was regulated by a thermocouple in the side wall of the furnace, while a Type S Pt-Pt 10% Rh thermocouple was inserted through the top lid and used to measure the temperature in the electrolyte. The conversion from emf [V] to degrees were done automatically by the logger. The design of the inside of the furnace and the top lid are shown in Figure 4.5 and 4.6. They also show how the electrodes, feeding tube and thermocouple were positioned in the furnace.

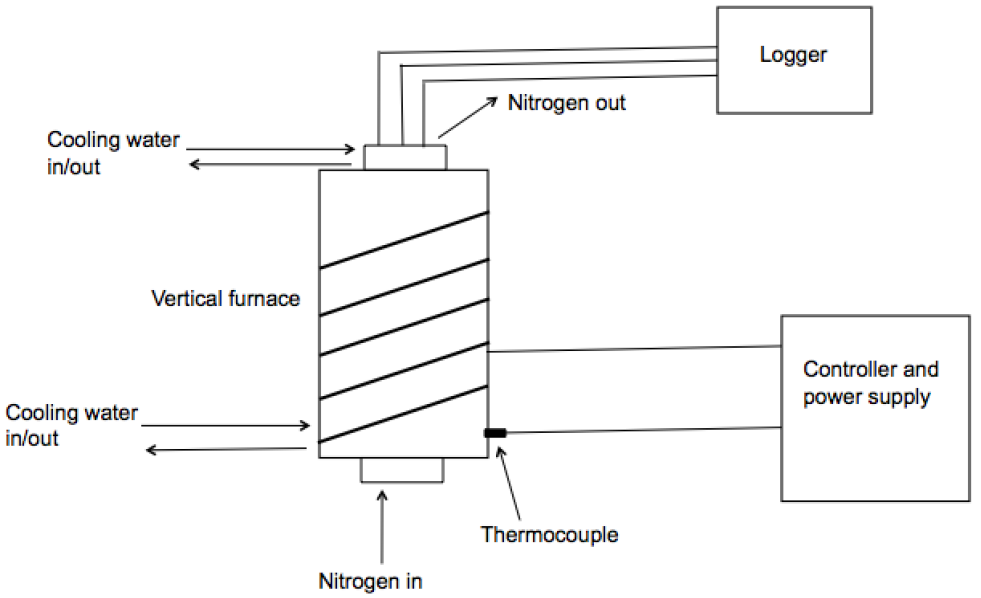

Figure 4.4: Sketch of the apparatus used during the measurements.

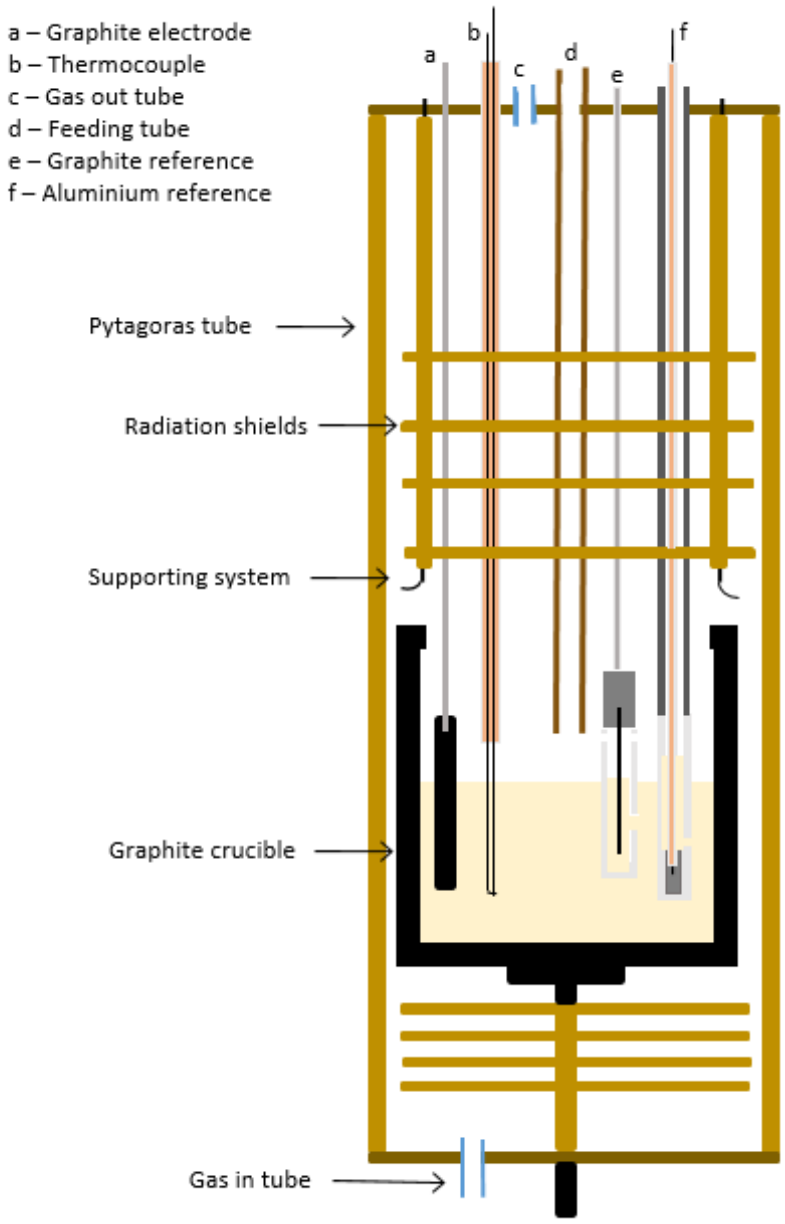

Figure 4.5: Sketch of the setup inside the furnace.

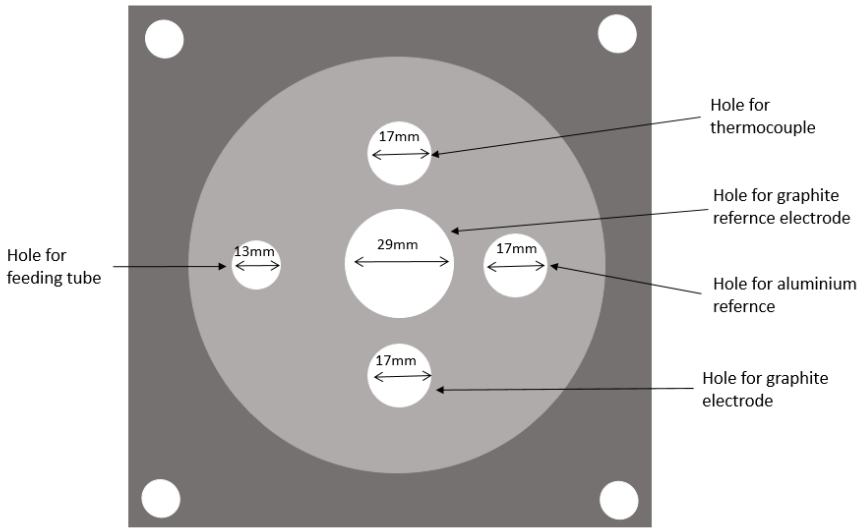

Figure 4.6: Design of top lid.

4.3 Implementation

A total of six experiments were performed. In the experimental procedure several adjustments were done. The experimental setup was as shown in Figure 4.5, but some changes were done in some of the experiment to fit the most necessary devices in the cell.

Experiment 1 was performed in order to test the robustness of the reference electrodes and the experimental setup.

In experiment 2 portions of 3 wt% Al_2O_3 were added to the melt, and in experiment 3 cryolite and varying amounts of alumina were added to the melt. The experimental setup was exactly as the one illustrated in Figure 4.5

In the experiment 4 CO_2 gas was fed to the cell in order to see how CO_2 influenced the emf measurements. Alumina, air and a piece of aluminium were added to the melt during the experiment.

The main purpose of experiment 5 was to add alumina without introduction of air to the melt. The graphite electrode used in former experiments was replaced by a totally immersed graphite electrode, as the one shown in Figure 4.2b.

In experiment 6 nitrogen gas was introduced into the melt and some of the alumina portions added were fully calcined.

Both reference electrodes were used in all of the experiments, except experiment 4 where only the aluminium reference was used. Measurements of the temperature in the melt were performed in all experiments, except experiment 6 due to space limitations. An overview of what were done in the different experiment is given in Table 4.1.

Table 4.1: Overview of what were done in the experiments.

Experiment	What was done
1	Testing of setup and reference electrodes
2	Additions of 3 wt% Al_2O_3
3	Additions of cryolite Addition of varying amounts of Al_2O_3
4	Introduction of CO_2 Addition of air Addition of aluminium while CO_2 is introduced
5	Addition of Al_2O_3 without introduction of air Use of totally immersed sensor
6	Addition of calcined Al_2O_3 Use of totally immersed sensor Introduction of N_2

The implementation of the experimental adjustments are described below.

4.3.1 Adding Alumina without Introduction of Air

A silicone hose connected to an alsint tube was used to add alumina to the cell without introducing any air. Alumina was placed in the hose and a plug with a tiny hole was plugged in the open end of of the hose. The outlet opening for the exit gas in the lid of the furnace was then closed, so the exit gas from the furnace had to pass through the hose with alumina to push the air out. The exit gas was flowed through the hose for approximately 15 minutes before the hose was closed completely. Then alumina was added from the silicone hose through the alsint tube.

4.3.2 Introduction of CO_2 Gas to the System

The nitrogen gas flowing through the furnace was turned off and CO_2 (Purity 5.3) gas was introduced through a alsint tube through one of the holes in the lid. Most of the time the gas was fed over the melt where the tube was placed 2-3 cm above the melt. The pressure was adjusted to achieve a stable potential in the cell. The amount of gas leaving the furnace was approximately two bubbles every second (bubbles in glucose which the gas leaving the furnace passed through before entering the fume suction. The gas was also bubbled into the melt for a shorter period. The alsint tube could only be immersed into the melt for a shorter period to prevent destruction of the tube, so bubbling into the melt was only performed for 10 minutes.

4.3.3 Introduction of Nitrogen Gas into the Melt

Nitrogen gas (purity: 5.0) was introduced into the melt through a steel tube placed 2-3 cm down in the melt. The gas flow was such that the frequency of the gas leaving the furnace was approximately two bubbles every second.

4.3.4 Use of Fully Calcined Alumina

Primary alumina was calcined over night (about 14 hours) at 1200 °C in a laboratory furnace.

Chapter 5

Results and Discussion

To improve readability, the results and discussion have been merged into one section.

A number of six laboratory experiments were performed in order to figure out if graphite materials can be used as sensors in emf measurements for determination of alumina concentration in cryolite melts. The temperature and the emf between graphite sensors and reference electrodes were measured as a function of time. Since either the use of the crucible or the graphite electrode gave quite similar results, only the results where the crucible were used are shown in this section, but there results where the graphite electrode are used is shown in Appendix C and D.

To achieve reliable alumina concentration measurement it is important that the changes in emf are related to change in alumina concentration and not other variations in the system that may impact the measurements. Since the system seems to be sensitive to other variables the focus has been to study the behaviour of the graphite sensor at different conditions to see what influence the measured potentials. The stability of the reference electrodes have also been considered. The main results of the experiments are listed in Table 5.1.

Table 5.1: Overview of the main results of the experiments.

Exp.	What was done	Results
1	Testing of setup and references	Adjustment in setup affect emf.
2	Additions of 3 wt% Al_2O_3	Decrease in emf. Immediate jumps/drops in emf after addition.
3	Additions of cryolite Addition of varying amounts of Al_2O_3	Immediate jumps/drops in emf after addition. Decrease in emf. Immediate jumps/drops in emf after addition.
4	Introduction of CO_2 Introduction of air Addition of aluminium with CO_2 present	Increase in emf. Increase in emf. Decrease in emf. Immediate jumps/drops in emf after addition.
5	Addition of Al_2O_3 without introduction of air Use of totally immersed graphite electrode	Not significant changes in emf form additions with air. Decrease in immediate drops/jumps in emf after addition.
6	Addition of calcined Al_2O_3 Use of totally immersed graphite electrode Introduction of N_2	Dampening of immediate drops/jumps in emf after addition. Decrease in immediate drops/jumps in emf after addition. No significant changes in emf.

5.1 Experiment 1−3

Experiment 1 was performed in order to test the robustness of the electrodes and the experimental setup. In experiment 2 and 3 alumina was added.

In experiment 1 it could be observed that adjustments in the experimental setup affected the emf measurements, but in a lesser extent. The adjustments could be removal of a plug from the top lid or installation of new electrodes or installation of the feeding tube. The robustness of the electrodes seemed to be good since no damage could be observed when they were removed.

Figure 5.1 and 5.2 show the results from experiment 2. The blue line in Figure 5.1 shows the variation in emf between the crucible and the graphite reference and

the blue line in Figure 5.2 shows the variation in emf between the crucible and the aluminium reference. The orange line expresses the variation in temperature. The red data points indicate at what time 3 wt% of alumina was added. A total of five additions were done, which gave a final alumina content of 16 wt%, when an initial concentration of 1 wt% is assumed. This value is above the saturation point of alumina which is approximately 13 wt% in this system according to FactSage. The results for the measurements where the graphite electrode is used as sensor is shown in Figure C.2 an 5.2 in Appendix C and gave quite similar results.

From theory, it was expected that the emf between a graphite sensor and a graphite reference should be approximately 0.14 V at 1 wt% of Al_2O_3 and approach to 0 V as the content of alumina approach saturation. It can clearly be seen from the graph in Figure 5.1 that the emf is not starting at 0.14 V and is not going towards 0 V, but the total decrease in emf is close to 0.14 V which do agree with the theoretical value for the total drop emf. The graph also seems to follow a logarithmic decreasing trend as the theoretical graph. More surprising were the sudden drops in emf immediately after alumina is added. It can be seen from the graph that every time alumina is added the emf suddenly drops with at least 0.10 V before the it starts to increase and stabilized again.

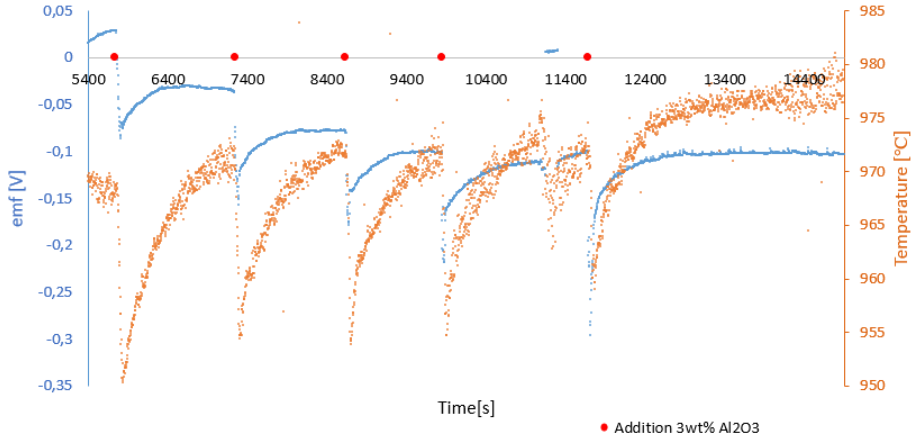

Figure 5.1: Emf between the crucible and graphite reference vs time (blue dots) in experiment 2. Temperature vs time (orange dots). The red data points indicate addition of 3 wt% alumina.

From the results of the emf measurements between the crucible and the aluminium reference, there can also be observed a decreasing trend after addition of alumina, but the measurement seems to be more sensitive to noise and the emf seems to jump instead of drop in the moment alumina is added. From Figure 5.2 it can be

seen that the emf decreases with approximately 0.10 V after the first addition (between ∼5800 and 7400 s) which is more than expected from theory. Since the emf has not stabilized before the addition was done it is not for certain that all of the reduction in emf is due an increasing alumina concentration. The emf continues to decrease until the fourth addition is done. According to the theory, shown in Figure 2.7, the decrease in emf should be around 0.10 V when the alumina concentration is increased 9 wt%. It can be seen from the experimental result that the emf is decreasing 0.15 V when 9 wt% of alumina is added which is higher than the theoretical value. This might be due to that the potential at the sensor had not stabilized before the addition or due to drifting of the electrodes. Drifting will be discussed in section 5.2. After the fourth addition the emf does not decrease as fast as earlier after the sudden increase. Why it does not follow the same trend after the fourth addition is difficult to explain.

The sudden drops or jumps in emf immediately after addition of alumina were surprising and it was decided to add smaller alumina doses in experiment 3 to see if the amount of alumina added affected the size of the drops or jumps in emf.

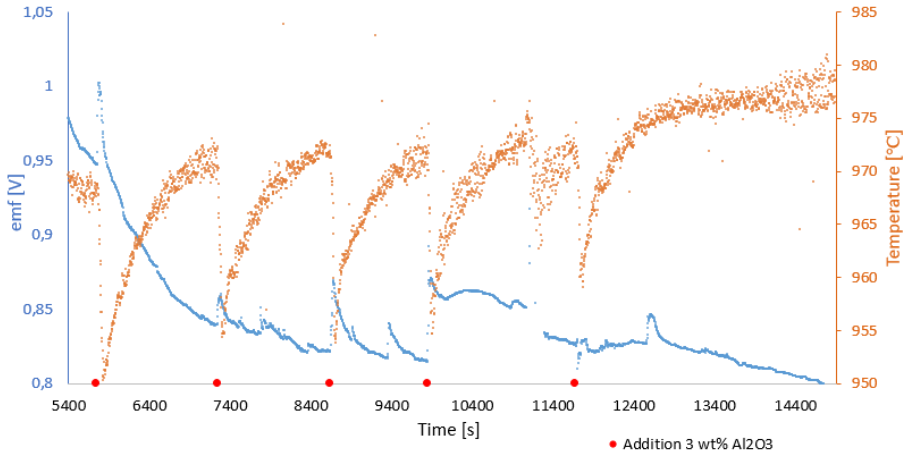

Figure 5.2: Emf between the crucible and aluminium reference vs time (blue dots) in experiment 2. Temperature vs time (orange dots). The red data points indicate addition of 3 wt% alumina.

In experiment 3 the same setup as in experiment 2 was used. The difference was that smaller portions of alumina were added in the first additions and that one portion of cryolite was added as well to see how that affected the potential. The results from experiment 3 differs from the results in experiment 2 at several points. The first thing that can be observed when looking at Figure 5.3 is that the total

decrease in emf between the crucible and the graphite reference, approximately 0.09 V, is lower than expected from theory (when looking at the value before the feeding tube is installed and cryolite is added). On the other hand, when looking at the emf between the graphite electrode and the graphite reference, see Figure D.4 in Appendix D, the total decrease is close to 0.14 V, which is the expected value. What causes the difference in emf when the graphite electrode is used as sensor versus when the crucible is used is uncertain and need to be investigated further. Another aspect that differs from the results of experiment 2 is that the emf between the crucible and the graphite reference is jumping immediately after some of the additions instead of dropping. The emf neither seems to stabilize between each addition as in experiment 2. It is approximately 20 minutes between each addition and according to literature completely dissolution of alumina should have take place within 20 minutes.

The emf measurement between the crucible and the aluminium reference in experiment 3, see Figure 5.4, is not that different from the same measurement in experiment 2. The emf starts at a higher value than in experiment 2, but it also ends at a higher value. The reduction is approximately 0.12 V from right before the first addition to when 8 wt% of alumina has been added. The fall in emf is around 0.12 V when 9 wt% alumina has been added in experiment 2. It can also be seen that the potential does immediate increase and not decrease as fast as for the other additions at $\sim$ 9900 s when the alumina concentration is increased to more than 10 wt% which also was the case in experiment 2.

From Figure 5.3 it can be seen that the potential between the crucible and graphite reference increased instantly when cryolite was added to the melt which it also did when alumina was added. It is not possible to say anything about the emf measurements between the crucible and aluminium reference when cryolite is added due to much noise in the measurements in the time interval (0-2000 s).

There exist no clear explanation for why the emf between a graphite sensor and the graphite reference drops in experiment 2 and jumps in experiment 3 immediately after alumina addition, while emf between a graphite sensor and the aluminium reference is jumping in both experiments. A possible cause of the different behaviors in the measurements when the graphite reference is used, could be due to the contact between the carbon surface (the graphite connector) on the top of the graphite reference with the atmosphere right above the melt which could cause changes in the measured emf.

The sudden jumps or drops in emf when alumina is added are hard to explain, but formation of CO and CO_2 due to airburn is believed to be one possible explanation. To get control of the CO/CO_2 partial pressures, CO_2 gas was introduced to the cell

in experiment 4. The presence of CO_2 can in this respect be regarded as a buffer in order to keep a constant partial pressure of the CO_2.

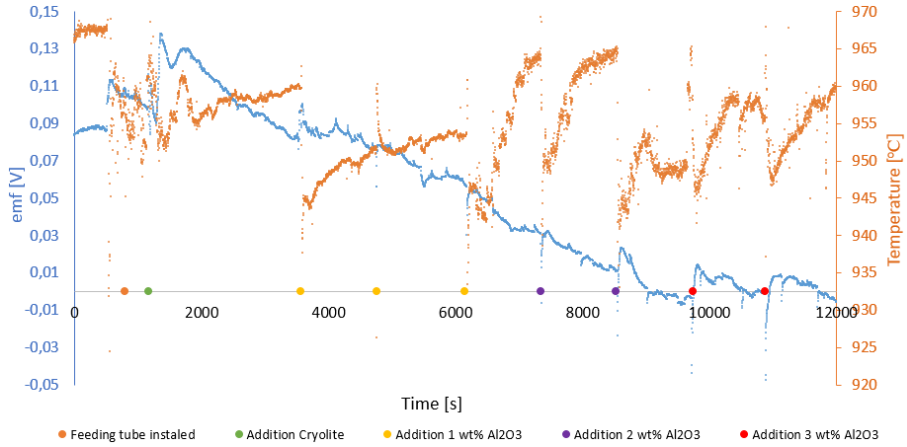

Figure 5.3: Emf between the crucible and graphite reference vs time (blue dots) and temperature vs time (orange dots) in experiment 3. The orange data point is installation of feeding tube, the green one is addition of cryolite to the melt. The yellow, purple and red data points are additions of 1 wt%, 2 wt% and 3 wt% of alumina, respectively.

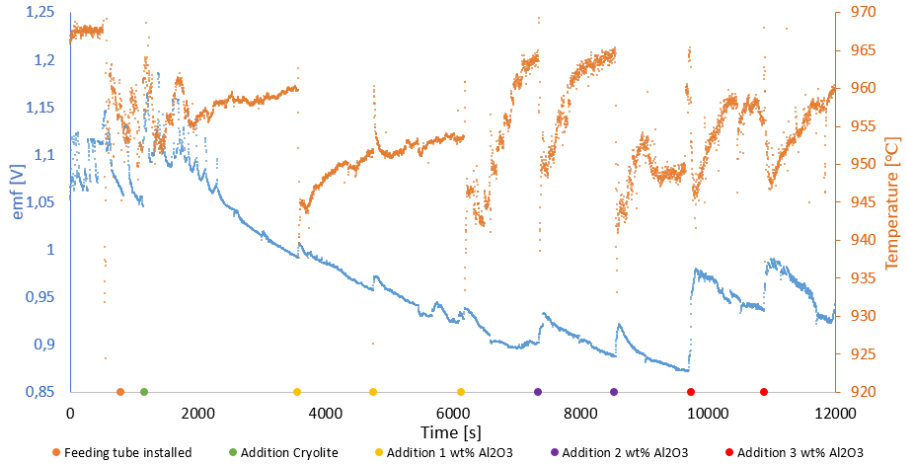

Figure 5.4: Emf between the crucible and aluminium reference vs time (blue dots) and temperature vs time (orange dots) in experiment 3. The orange data point is installation of feeding tube, the green one is addition of cryolite to the melt. The yellow, purple and red data points are additions of 1 wt%, 2 wt% and 3 wt% of alumina, respectively.

5.2 Drifting in the Potential

Drifting was a recurring phenomenon in the experiments, and this will be discussed now before the discussion of experiment 4.

In all of the emf measurements where the aluminium reference have been used, drifting or fluctuations are observed. Drifting and fluctuation mean that the potential is changing with time even though no changes in the bath composition were done. When the drifting of potential is going in the negative direction it means that the graphite sensor is drifting in the negative direction or that the reference is drifting in positive direction. In all of the experiments the potential drifts in the negative direction.

Dissolved metal, both sodium and aluminium, might gradually react with CO and CO_2 and therby decrease the partial pressures of them which will lead to a decreasing potential at the graphite sensor and contribute to a decreasing emf according to equation (2.30).

One possible explanation to the jumps/drops in emf immediately after addition of alumina is that air added together with alumina causes airburn and thereby formation of CO and CO_2 which will increase the potential at the graphite sensor. If CO and CO_2 are consumed by metal one will get very low concentrations of them further into the experiment, and one might speculate if that may lead to larger jumps in emf immediately after alumina addition further into the experiments. Larger jumps in potential in conjunction with addition of alumina farther into the experiments can be seen in both experiment 2 and 3, but in experiment 3 the amount of alumina added increased farther into the experiment which also may impact the magnitude of the jumps.

According to Grjotheim et al. [6] one explanation of the drifting of the aluminium reference in positive direction might be problems with the contact wire inside the reference since the wire becomes corroded as some metal will dissolve in aluminium and a solid intermetallic compound is formed at the surface of the wire. Other explanations may be dissolving of metal into the melt or change in the composition of the melt adjacent to the electrode.

Sterten et al. [20] showed that the emf values for a cell consisting containing an aluminium reference decreased with decreasing NaF/AlF_3 ratio. Some of the aluminium inside the aluminium reference may leak into the melt and reacts with NaF to form AlF_3, see equation (5.1). This will decreases the NaF/AlF_3 ratio and thereby the potential.

$$Al(l) + 3NaF \rightarrow AlF_3 + 3Na \tag{5.1}$$

It is expected that the activity of aluminium will decrease with time due to a decreasing purity of the metal. According to equation (2.30) will a decreasing activity of aluminium lead to a decrease in emf.

Other aspects that may cause drifting in potential may be changes in the bath composition due to vaporization, equation (2.3), reactions with impurities form oxides, equation (2.4) or reactions with moisture, equation (2.5) [21]. But both vaporization and reactions with impurities and moisture contribute to a increase in potential which is only observed in a small number of the experiments and in those cases close to the end of the experiment.

Figure 5.5, 5.6 and 5.7 illustrates variations in emf with time for the three experiments with longest duration time, experiment 4, experiment 5 and experiment 6, respectively. In experiment 4 no additions of any powders were done before the very end of the experiment, after ∼160000 s seconds. The only adjustment done was introducing CO_2 gas at ∼5000-7000 s and ∼71000-90000 s. It can be seen that the emf drifts in the interval from ∼10000-71000 s when no adjustments are done in the cell, but at the interval between∼90000-160000 s when noting is adjusted the emf seems to be relatively stable. So the drifting seems to stop after a certain time. This may be due to no more leakage of Al out of the reference and thereby no more decrease in amounts of CO and CO_2 and no more decrease of the aluminium activity.

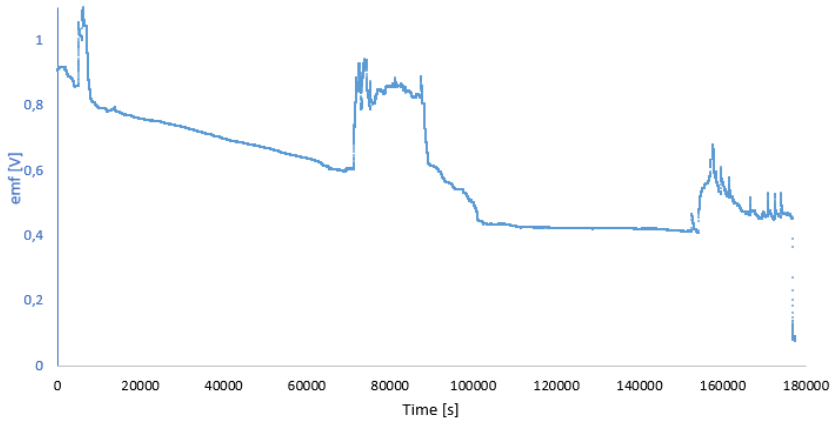

Figure 5.5: Emf between crucible and aluminium reference vs time in experiment 4.

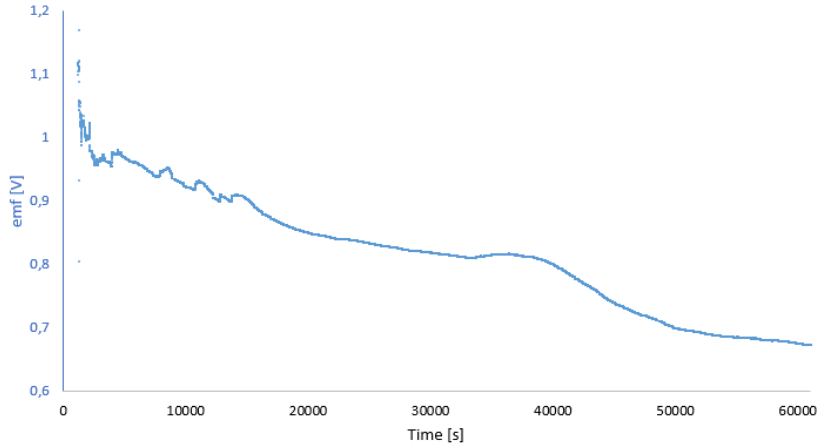

Figure 5.6: Emf between crucible and aluminium reference vs time in experiment 5.

The drifting rate seem to decrease with time in experiment 5 and 6 as well, but since additions of alumina have been done in these experiments (until ∼15000 s in experiment 5 and until 12000 s in experiment 5) it is difficult to determine if the decrease of emf is due to drifting. It is also difficult to comment on the drifting in experiment 2 and 3 due to shorter duration time and a several additions of alumina.

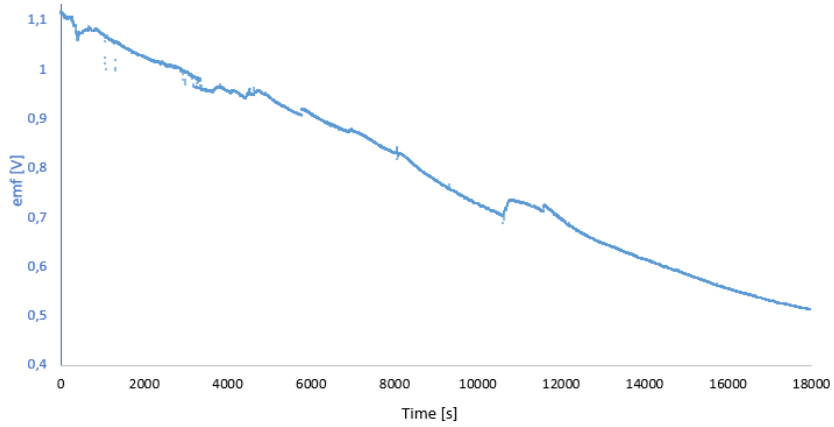

Figure 5.7: Emf between crucible and aluminium reference vs time in experiment 6.

The measurements with the use of the graphite reference does not seem to be affected by drifting to the same extent. The emf measurements of experiment 5 can be seen in Figure 5.8, but due to several alumina additions between 3000-15000 s the decrease in emf is not only due to drifting. Since the all of the electrode are

placed in the same melt leakage from the aluminium reference will affect the emf measured between the graphite sensor and the graphite reference as well. A reason for the drifting of the graphite reference in positive direction may be decrease of the alumina concentration inside the reference due to leakage of the saturated melt out of the reference and penetration of bath with low alumina content into the reference. This may cause a reduction of the activity of Na_2O inside the reference and then the emf will decrease according to equation (2.17).

For both reference electrodes it may be of interest to use a boron nitride tube without hole for electrolyte penetration in order to prevent leakage from the reference electrodes to the bath. Extra thin walls of the boron nitride or some kind of porous plugs instead of holes are then needed in order to keep the ion migration.

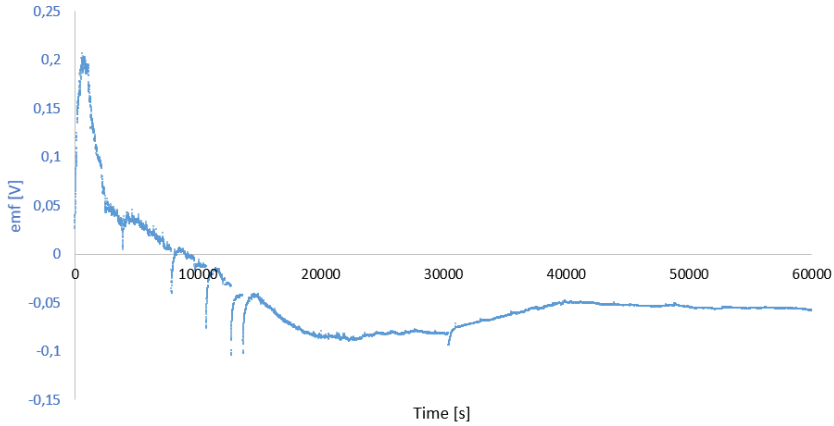

Figure 5.8: Emf between crucible and graphite reference vs time in experiment 5.

5.3 Variation of Temperature

The temperature was measured in all experiments, except experiment 6.

Since the temperature seems to follow the same trend in all of the experiments it is not included in all of the illustrations of the results in order to improve readability. The temperature tended to drop about 20 °C when powder at room temperature was added, and it did not seem like the amount of powder did affect the drop in temperature significantly.

From Figure 2.4, showing how the potential is varying with an increasing temperature according to theory, it was expected that the change in temperature would not

influence the potential with more than a few mV. It was also expected that the magnitude of the variation in potential due to variation in temperature did vary with the content of alumina in the melt. A temperature drop of 20 °C at an alumina content of 1 wt% should cause a drop in potential of 0.004 V and at an alumina content of 12 wt% it should cause a potential drop less than 0.001 V. The temperature variations in experiment 2 are shown in Figure 5.1. From all experiments it can be seen that the potential drops are larger than the theoretical expected potential drops due to change in temperature after alumina. The results from experiment 3, Figure 5.3, do not show the same sudden drop in potential when alumina is added and since the potential is dropping and jumping at approximately the same time it is impossible to say if variation in temperature is the cause of any of the change in potential. But for almost all additions where the potential drops in experiment 3, it drops with more than a few mV, so it is clear that change in temperature cannot be the cause of the sudden drop in potential itself. It is also worth noticing that the potential is not dropping at all in the measurements where the aluminium reference is used in experiment 2 and 3 except at the fifth addition in experiment 2 where it is dropping with approximately 0.02 V. Anyway, this drop is too large to be caused by the temperature drop itself.

5.4 Switching off/on the Furnace Controller

The furnace controller was turned off in short intervals in experiment 4 in order to see if electric noise from the furnace controller influences the emf measurements. Figure 5.9 illustrates what happens when the furnace is turned off. It can be observed a jump in the temperature curve when the furnace is turned off and an other one approximately 59 seconds after the furnace is turned on again. The jumps in temperature are approximately 10-15 °C. The temperature is also steadily decreasing in the time interval between the furnace is turned off and back on again. A decreasing temperature when the furnace is turned off was expected, but the immediate jumps in temperature when the furnace is turned off and a short time after it was turned back on is difficult to explain, but might to be due to induced voltage due to the furnace.

No visible change in emf can be seen in the moment the furnace is turned off, but as the temperature starts to decrease, the emf starts to increase slightly. It can be seen that the temperature and the emf follow the opposite trend. The temperature do decrease with approximately 30 °C. The emf is increasing with about 0.020 V which is higher than what is expected for a decrease in temperature of 30 °C. According to equation (2.31) a reduction from 980 °C to 950 °C will increase

the emf with less than 0.001 V. So that the increase in emf is due to changes in temperature or impact from the controller is uncertain. The purpose of switching off/on the furnace was to see if it caused jumps in potential, which it did not. So there are no reasons to believe that the controller of the furnace will influence the concentration measurements.

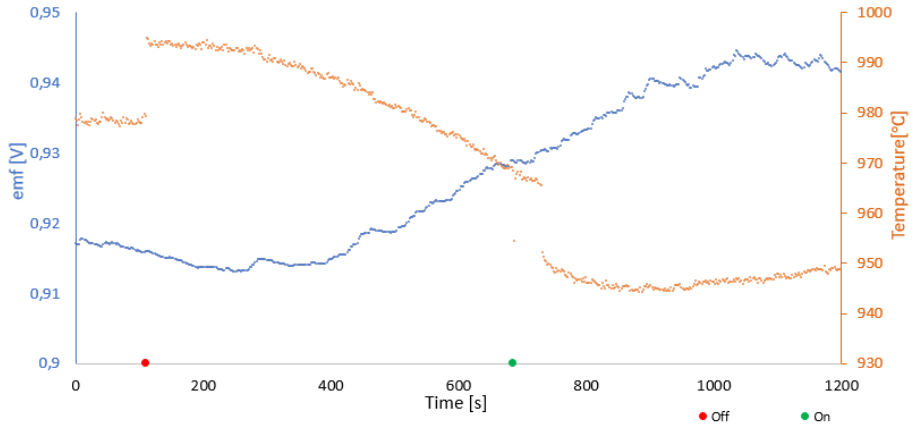

Figure 5.9: Potential and temperature as a function of time when the furnace/controller is turned off and on. The blue curve illustrates the emf of carbon crucible versus aluminium reference electrode and the orange curve represents the temperature.

5.5 Introduction of CO_2

In experiment 4, CO_2 was introduced to the system. Due to limited holes in the lid and radiation shields, the aluminium reference was the only reference electrode used in this experiment.

Introduction of air in conjunction with added alumina may be one reason for the jumps/drops in potential immediately after addition. Various reactions may occur between carbon, carbon monoxide and oxygen from air [7]:

$$C(s, anode) + O_2(g) = CO_2(g) \tag{5.2}$$

$$C(s, anode) + O_2(g) = 2CO(g) \tag{5.3}$$

$$2CO(g) + O_2(g) = 2CO_2(g) \tag{5.4}$$

These reactions may alter the partial pressures of CO and CO_2 in the cell and at the sensor and cause an increase in emf as can be understood by study equation (2.24).

A constant flow of CO_2 into the cell is believed to prevent large variations in the partial pressures of CO and CO_2. The added CO_2 will establish a buffer system with respect to small amounts of air added the cell. CO_2 gas was used due to HSE considerations. CO_2 is in equilibrium with CO and will work as a buffer for both species.

Figure 5.10 shows variation in emf when CO_2 gas is fed. When CO_2 is introduced to the system the emf increases considerably. The response was very quick; it increased immediately after the CO_2 gas was turned on. This immediate increase in emf indicate that formation of CO and CO_2 might be a reason for the immediate increase of the emf when alumina is added. It also substantiates that the equilibrium between CO above melt and adsorbed on the electrode is fast as assumed in theory. It can also be seen from the results, Figure 5.11, that a higher flow rate of CO_2 gave an even higher increase in potential. Figure 5.10 shows that the potential increases with approximately 0.15 V when the CO_2 gas was turned on, and even more after $\sim$ 6300 s when the flow of CO_2 gas flow was increased. The fluctuations in the emf curve are due to adjustment of the gas flow.

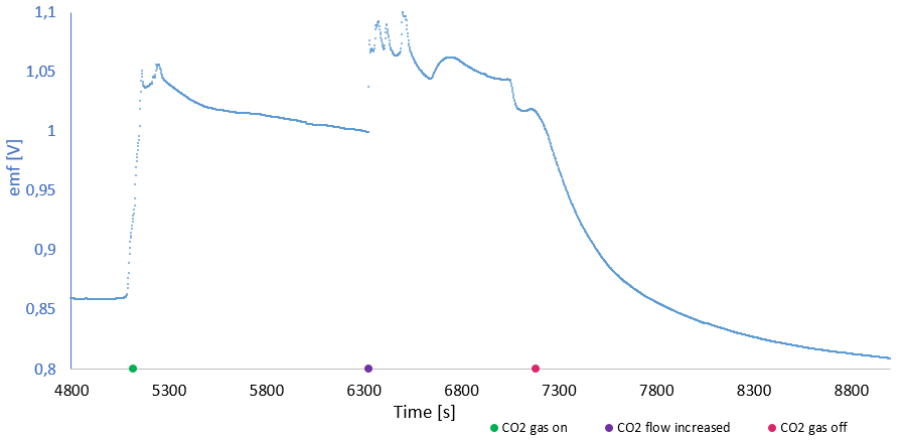

Figure 5.10: Emf between crucible and aluminium reference vs time when CO_2 is introduced to the cell.

At the dark grey point on the x-axis in Figure 5.11 the gas feeding tube is lowered into the melt (∼73200-73600 s) which leads to a decrease in emf. When the gas feeding tube is raised from the melt, the emf increases again. The decrease in potential when CO_2 was bubbled into the melt was opposite of what was expected, since feeding of CO_2 into the melt should give even more CO_2 and CO in the melt. It may be that some CO_2 gas did penetrate into the reference when CO_2 was fed directly into the melt, which may have caused a increase in potential at the reference and thereby decrease in emf. It might also indicate that changes in gas composition above the melt do affect the measurements in a significant manner.

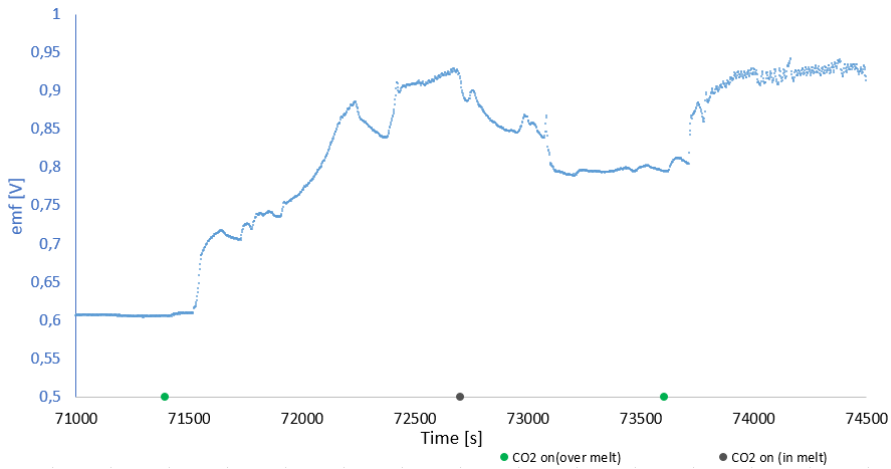

Figure 5.11: Emf between the crucible and aluminium reference vs time when CO_2 first flows above the melt and then into the melt.

Figure 5.12 and 5.13 shows the systems sensitivity to the contact with the atmosphere outside the furnace. One of the rubber plugs closing one of the holes in the lid was taken out such that the environment inside and outside the furnace got in touch with each other. Figure 5.12 shows the changes in emf when a plug are removed when CO_2 is not fed to the furnace, while Figure 5.13 shows the variations in emf when CO_2 gas is fed to the furnace. From Figure 5.12 it can be seen that the emf increased about 0.015 V. When CO_2 was fed to the furnace no changes in emf are observed. The experiment was repeated several times and gave the same results each time.

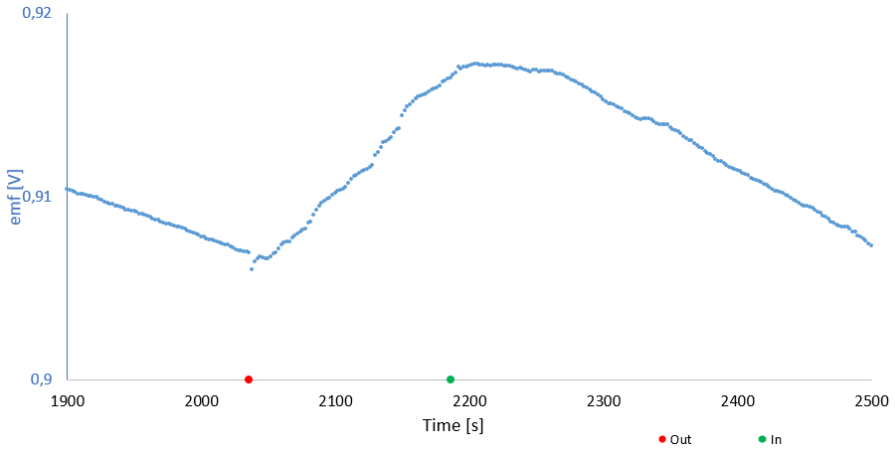

Figure 5.12: Emf between the crucible and aluminium reference vs time when one plug in the top lid is removed and inserted again when no CO_2 is introduced.

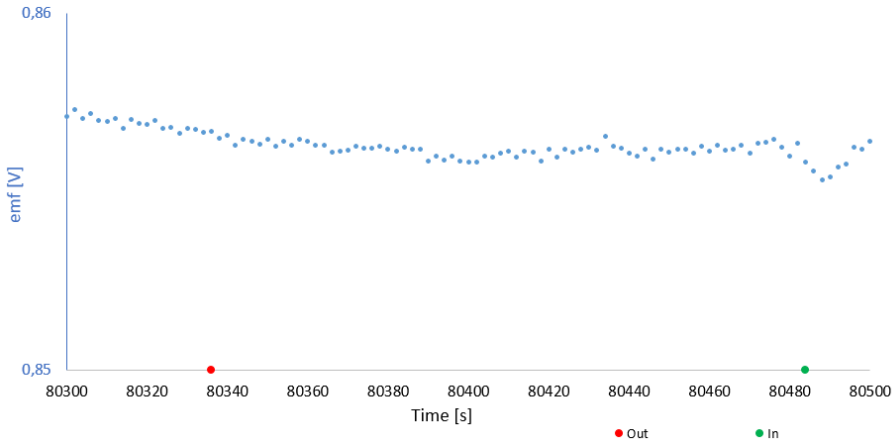

Figure 5.13: Emf between the crucible and aluminium reference vs time when one plug in the top lid is removed and inserted again while CO_2 is fed to the furnace.

Even though CO_2 is fed to the system the sharp jumps in emf immediately after alumina addition are not hindered, which can be seen from Figure 5.14. Even though the introduction of CO_2 gas hindered change in potential when taking out one of the plugs in the top lid, CO_2 did not change the system's reaction when alumina was added. This difference is not understood, but it might be dependent of the amount of air added. In experiment 5, alumina is added without introduction of air to see how that affected the immediate jumps in potential.

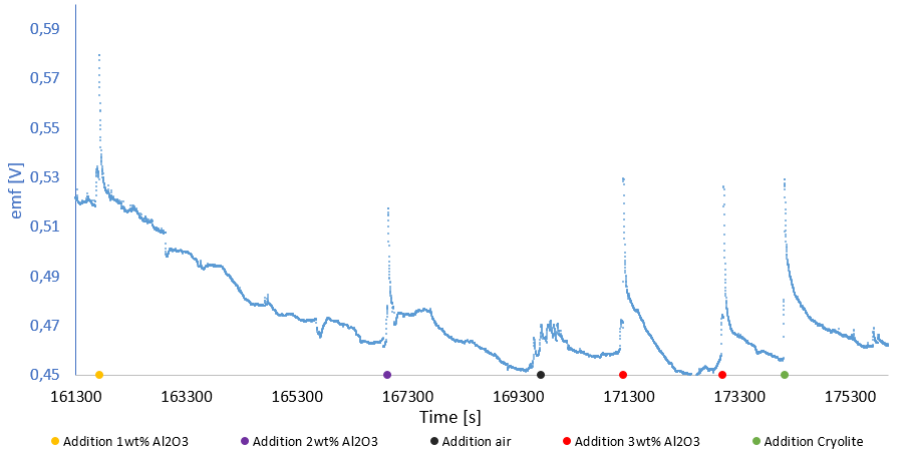

Figure 5.14: Emf between crucible and aluminium reference vs time while CO_2 is fed. The yellow, purple and red data points are additions of 1 wt% alumina, 2 wt% and 3 wt% of alumina, respectively. The green data point represents addition of cryolite and the black data point represents addition of air.

5.6 Addition without introduction of air

In experiment 5 alumina was added without introduction of air from the atmosphere.

One explanation for the immediate changes in potential in the moment alumina was added was that air which was draggen by the powder down to the melt causes an immediate change of the potential. As described in equation (5.2), (5.3) and (5.4) oxygen may increase the partial pressures of CO and CO_2 which will cause a positive change in potential.

By comparing the additions done by not introducing air and when air is introduced in Figure 5.15, no significant differences can be observed in the emf between the crucible and the aluminium reference. Since the emf already is increasing when alumina is added at $\sim$ 4000 s it is hard decide the magnitude of the immediate change in potential due to alumina addition. It might look like it jumps from 0.84 V to 0.90 V which make up an increase of 0.060 V. At $\sim$ 8000 s, when alumina is added without introduction of air, the immediate change in emf is also around 0.060 V. Based on this result it does not seem like addition without introduction of air make any difference.

When it comes to how additions without introducing any air affects the difference

in potential between the crucible and the graphite reference, see Figure 5.16, it is also here difficult to compare the addition done ”with air” with the additions done ”without air” since the emf is already changing when the first addition is done. The additions without introduction of air gives an immediate drop in emf of approximately 0.02-0.03 V which is lower than the drops in experiment 2 which was approximately 0.10 V.

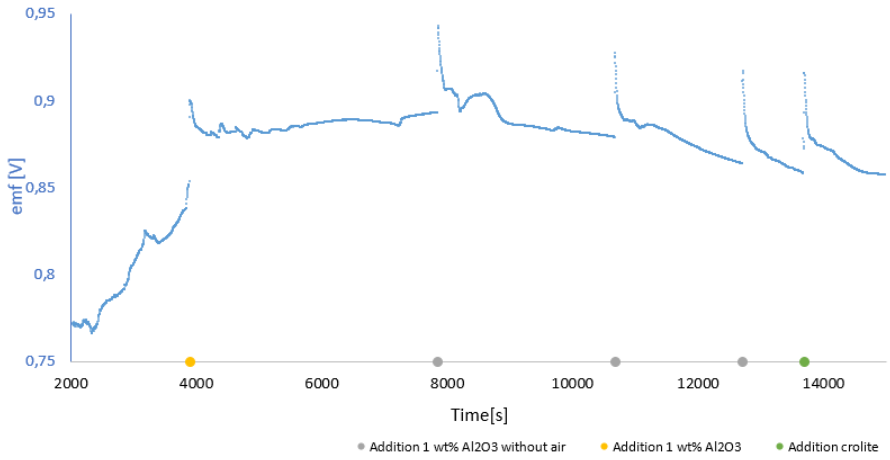

Figure 5.15: Emf between the crucible and the aluminium reference when portions of primary alumina (yellow data point) and one portion of cryolite (green data point)were added. Three of the additions were done without introduction of air (grey data point).

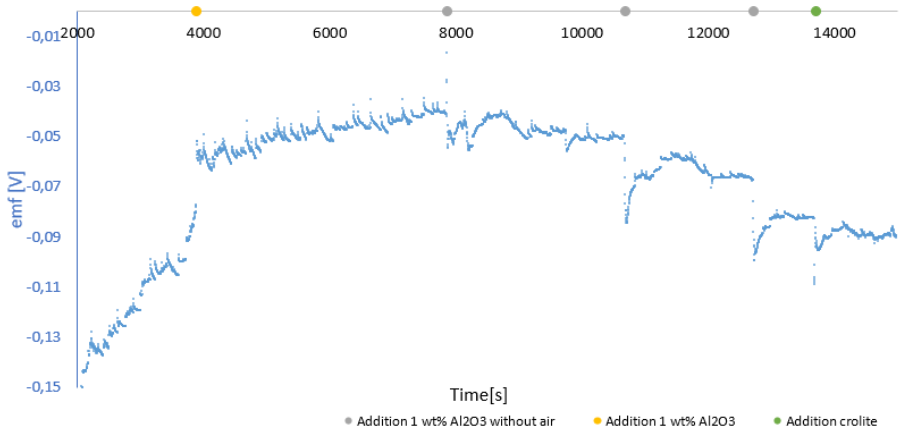

Figure 5.16: Emf between the crucible and the graphite reference when portions of primary alumina (yellow data point) and one portion of cryolite (green data point) were added. Three of the additions were done without introduction of air (grey data point).

Since an increase in the amount of CO and CO_2 would increase the potential it is not believed, according to these results, that addition of oxygen is the reason for the drop in potential, and one should believe that addition without air introduction should cause larger drops in potential between the crucible and the graphite reference since CO and CO_2 do contribute to a more positive potential. But there may exist some gibbsite and some air in the pores of the alumina grains that would react with the melt and cause the drops/jumps in emf.

It was also tried to add air to the atmosphere above the melt by the use of a pipette balloon. The balloon was pumped several times in a row. The air gave an increase in emf of 0.01-0.02 V as shown in Figure 5.17. The air addition was done in experiment 4 when CO_2 already was introduced to the system, which may have given a lower impact on the emf than if CO_2 was not present. Oxygen is more oxidizing than CO_2 so some increase in potential is expected anyhow.

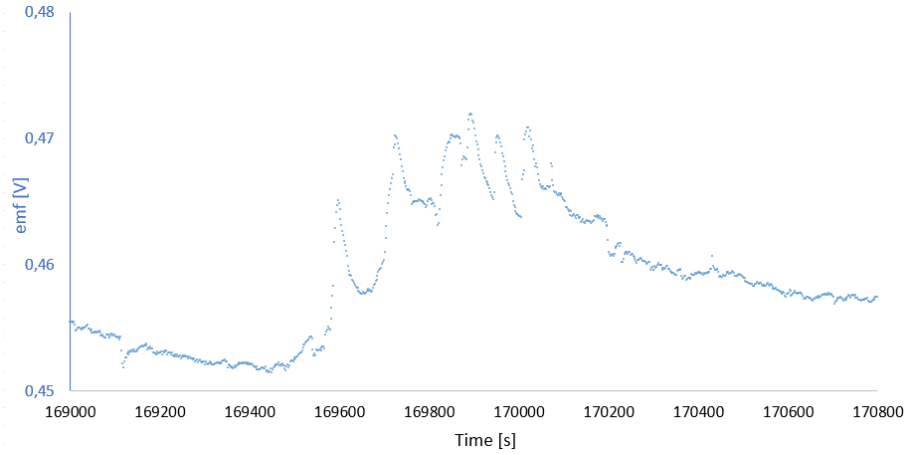

Figure 5.17: Measured potential between the crucible and the aluminum reference electrode when air was added to the cell by the use of a pipette balloon.

5.7 Use of Totally Immersed Graphite Sensor

A totally immersed graphite electrode was used as sensor in experiment 5 and 6. This sensor was tested to see if the atmosphere above the melt affected the measured emf. It can be seen from the results that the totally immersed sensor dampens the sudden jumps in emf between the sensor and the aluminium reference when alumina is added, which might indicate the atmosphere above the melt do influence the potential at the electrodes.

In experiment 5, the potential between the crucible and the aluminium reference, see Figure 5.15, jumps about 0.060 V while the potential between the totally immersed electrode and the aluminium reference, see Figure 5.18, gives a jump in potential that is much lower, around 0.01 V. These results might indicate that changes in the atmosphere right above the melt do influence the emf measurements.

Even though these results indicate that changes in the gas composition above the melt do influence the emf, it is a bit odd that a change above the melt may make a difference of this magnitude since it is only a small part of the electrode that is above the melt compared with the part in the melt. Exactly what kind of change that causes the difference in potential when the totally immersed electrode is used is not clear since several factors are involved such as alumina dust, gas generation when alumina is added, air or other species that alumina brings with it down to the surface of the melt. In order to try to figure out what kind of species that caused the jumps in potential, it was tried to add fully calcined alumina to see if e.g. moisture or gibbsite in the alumina powder was the cause, see section 5.9.

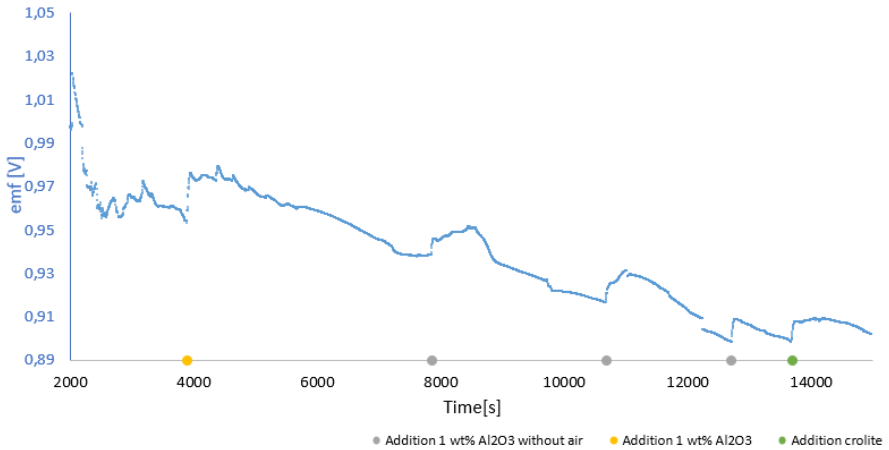

Figure 5.18: Emf between a totally immersed graphite electrode and the aluminium reference when portions of primary alumina (yellow data point) and one portion of cryolite (green data point) were added to the bath. Three of the additions was done without introduction of air (grey data point).

On the other hand, when studying the results where the graphite reference is used, one can not observe the same difference between using the crucible or a totally immersed electrode as graphite sensor. That can be seen by comparing the results in Figure 5.19 and 5.16 which are both from experiment 5, but with the use of different graphite sensors. Actually, the immediate drops in emf after addition are

greater in the measurements where the totally immersed electrode in most cases.

There exist no clear explanation of why the measurements done with aluminium reference seems to be more sensitive to changes in the atmosphere above the melt than the measurements done with the graphite reference. One possible explanation may be that the connector between the graphite rod and the steel rod in the graphite reference is made of graphite and this part of the reference is in contact with the atmosphere above the melt. Since both the graphite reference and the crucible are exposed to changes in the atmosphere above the melt, there is reasons to believe that changes in the atmosphere will not give substantial impact on the potential difference between them. This may also explain that the immediate drops in potential are somewhat greater for the emf between the totally immersed sensor and the graphite reference since only one of the electrodes has contact with the area above the melt.

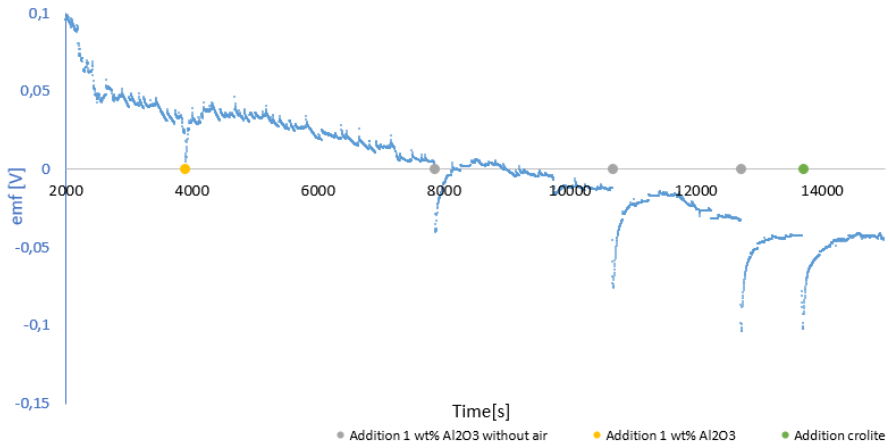

Figure 5.19: Emf between the totally immersed graphite electrode and the graphite reference when portions of primary alumina (yellow data point) and one portion of cryolite (green data point) were added. Three of the additions was done without introduction of air (grey data point).

5.8 Introduction of Nitrogen to the melt

Nitrogen gas was bubbled in the melt in experiment 6.

The purpose of bubbling nitrogen into the melt was to ensure an even distribution of eventual air entering the melt as a consequence of powder addition and simultaneously force gaseous species out of the melt as fast as possible after addition. The nitrogen gas does also contain small amounts of oxygen which might contribute to stabilize the potential (purity: 5.0). It cannot be seen any immediate effects on the emf when the nitrogen gas was introduced into the melt. Bubbling of nitrogen gas into the melt did not seem to prevent the sudden drops or jumps (depending on which reference which was used) in emf when alumina was added. From Figure 5.20 can be seen that both the additions of primary alumina at $\sim$4700 and $\sim$5900 s gives a jump in the emf between the crucible and the aluminium reference of almost 0.20 V. A jump of almost 0.20 V is almost twice as much than what has been measured in the other experiments. It can also be observed that the emf between the crucible and the graphite reference is jumping immediately after addition for these additions as well, so maybe nitrogen actually affected opposite of expected.

5.9 Use of Fully Calcined Alumina

A batch of fully calcined alumina was made by calcining primary alumina for 12 hours at 1200 °C. Fully calcined alumina was added to the melt in order to see how the removal of the hydrate affected the measured emf. It was expected that by calcining the alumina the amount of gas generated when alumina was added would decrease and thereby affect the emf to a lesser extent.

Figure 5.20 and 5.21 show the emf measured between the crucible and the aluminium reference and the totally immersed graphite reference and the aluminium reference, respectively. By comparing the addition of 1 wt% primary alumina and 1wt% fully calcined alumina in Figure 5.20 it can be seen that the addition of fully calcined alumina causes a much smaller jumps in emf in the moment alumina is added. When 1 wt% of primary alumina is added the emf increases with around 0.170 V while when fully calcined alumina is added the emf increases with 0.015 V. Due to the large difference in emf, there are reasons to believe that moisture or gas evolution from hydroxyls in the primary alumina causes instant growth in emf.

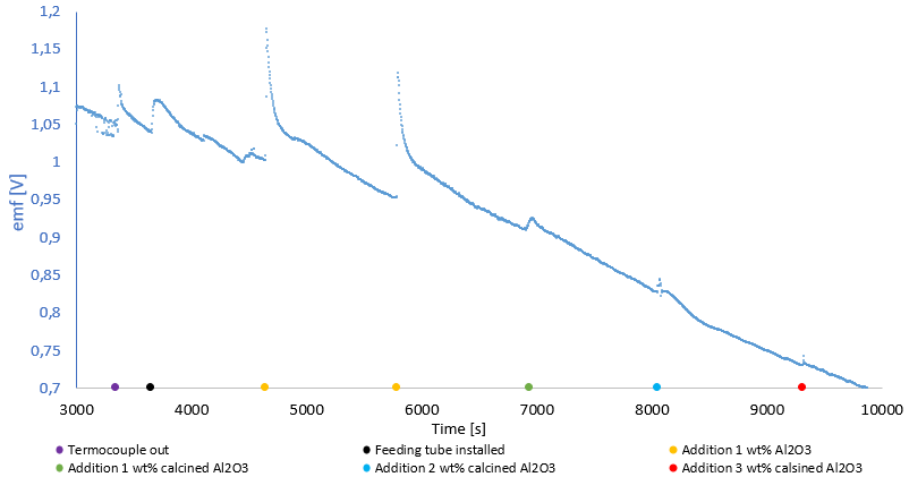

Figure 5.20: Emf between the crucible and the aluminium reference. Portions of 1 wt% primary alumina (yellow data point) and portions of fully calcined alumina (green=1 wt%, blue=2 wt%, red=3 wt%) were added. The purple data point is removal of the thermocouple and the black data point are installation of the feeding tube. Nitrogen was bubbled into the melt during the experiment.

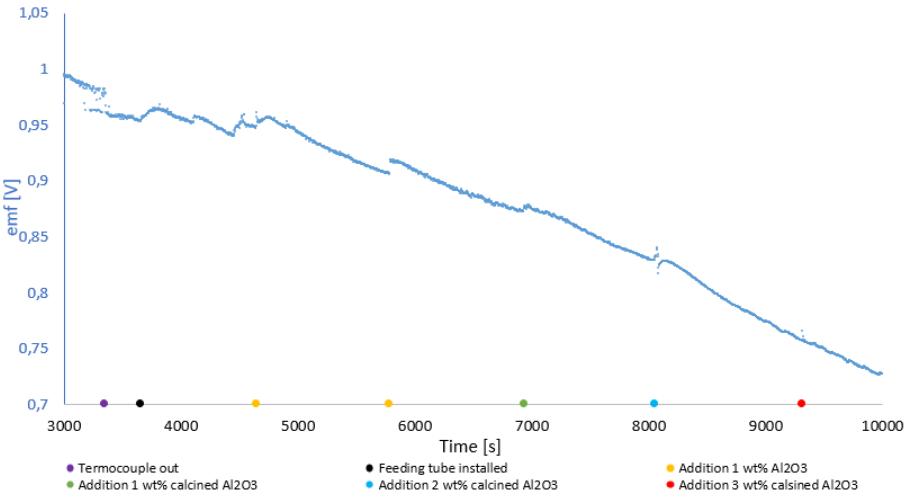

Figure 5.21: Emf between a totally immersed graphite electrode and the aluminium reference. Portions of 1 wt% primary alumina (yellow data point) and portions of fully calcined alumina (green=1 wt%, blue=2 wt%, red=3 wt%) were added. The purple data point is removal of the thermocouple and the black data point are installation of the feeding tube. Nitrogen was bubbled into the melt during the experiment.

Osen et al. [22] reported that the structural hydroxyl in primary alumina is one of the main sources of water. Structural hydroxyl is incorporated in the crystal lattice in aluminas and is removed when alumina is heated above 1000 °C and α-alumina is formed. Fluorides present in the bath and in the vapour phase will react with moisture according to the following reactions:

$$AlF_3(diss\,or\,g) + 3H_2O(g) = 6HF(g) + Al_2O_3(s\,or\,diss) \tag{5.5}$$

$$3NaAlF_4(g) + 3H_2O(g) = 6HF(g) + Al_2O3(s) + Na_3AlF_6(s). \tag{5.6}$$

Hyland et al. [23] argued that structural hydroxyl contributes to HF formation in two ways. The first one is when alumina enters the bath and structural hydroxyl reacts with fluorides instantaneously to form HF. Secondly, a more steady state HF formation from the structural hydroxyl. The jumps in emf when alumina is added in figure 5.20 happens immediately and fits with the statement by Hyland et al. that fluorides may react with structural hydroxyls instantaneously. But exactly how HF contributes to increase the potential need to be investigated further.

The emf measured between the crucible and the aluminium reference differs from the emf measured when the totally immersed electrode is used. By studying the graph in 5.21 there cannot be seen large jumps in emf when 1 wt% of primary alumina is added (at ∼5000 s and ∼6000 s) as was observed in Figure 5.20. Since these jumps of 0.17 V in emf for 1 wt% Al_2O_3 only can be observed in the case where the sensor is in contact with the atmosphere it might seem like a change in the atmosphere above the melt contributes to sudden jumps in emf, and that fluorides in the gas phase do react with moisture from alumina. As described in equation (5.5) and (5.6) the change in gas composition may be due to an increasing level of HF(g), but also a decreasing level of AlF_3(g) and $NaAlF_4$(g).

By comparing the emf in the moment where 1wt% fully calcined alumina was added in Figure 5.20 and 5.21 it can be seen that the emf between the crucible and the aluminium reference increases with 0.015 V while the potential between the totally immersed electrode and the aluminium reference increases with 0.006 V, so even though fully calcined alumina is used it may seem like the gas composition above the melt changes, possibly due to CO and CO_2 formation as described earlier, and that immediate changes in the bath only give rise to a very small change in emf.

It is also worth noticing that the changes in emf when the thermocouple is removed and the feeding tube are installed are smaller when the totally immersed electrode is used.

Figure 5.22 and 5.23 shows the emf measured between the crucible and the graphite reference and the totally immersed graphite electrode and the graphite electrode, respectively. In the measurements where the crucible is used as the sensor the emf suddenly jumps when primary alumina is added, while it is dropping when fully calcined alumina is added. The reason for the jumps in emf immediately after addition of primary alumina is difficult to explain, but might be due to changes in the gas above the melt due to reaction with moisture or gibbsite in the primary alumina since these jumps cannot be observed when fully calcined alumina is added or for in the measurements where the totally immersed electrode is used, Figure 5.23.

The measurements where the crucible is used and the measurements where the totally immersed electrode is used seem to give drops of the same magnitude when fully calcined alumina is added, which might indicate that these drops in emf are due to changes in the bath. Emf between the crucible and the graphite reference seem to drift in the negative direction after the last addition of primary alumina. This drift may be due to changes in the gas above the melt since the emf between the totally immersed electrode and the graphite reference does not seem to decrease to the same extent.

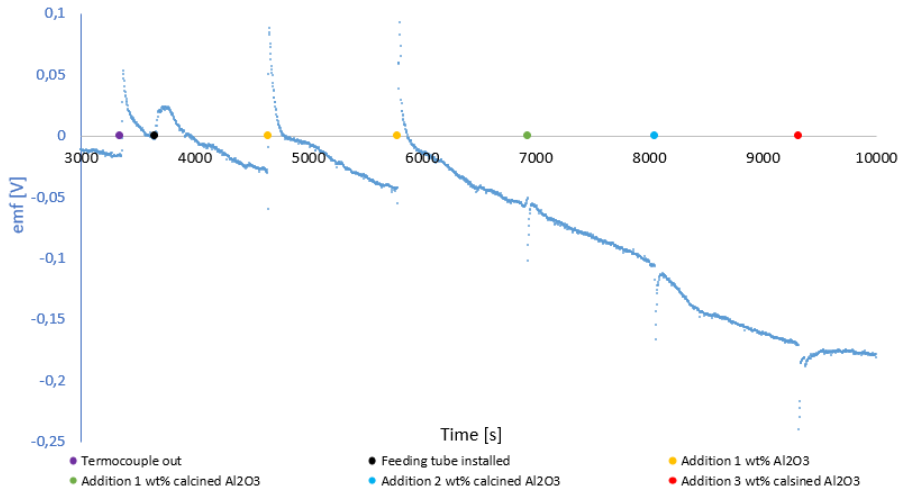

Figure 5.22: Emf between the crucible and the graphite reference. Portions of 1 wt% primary alumina (yellow data point) and portions of fully calcined alumina (green=1 wt%, blue=2 wt%, red=3 wt%) were added. The purple data point is removal of the thermocouple and the black data point are installation of the feeding tube. Nitrogen was bubbled into the melt during the experiment.

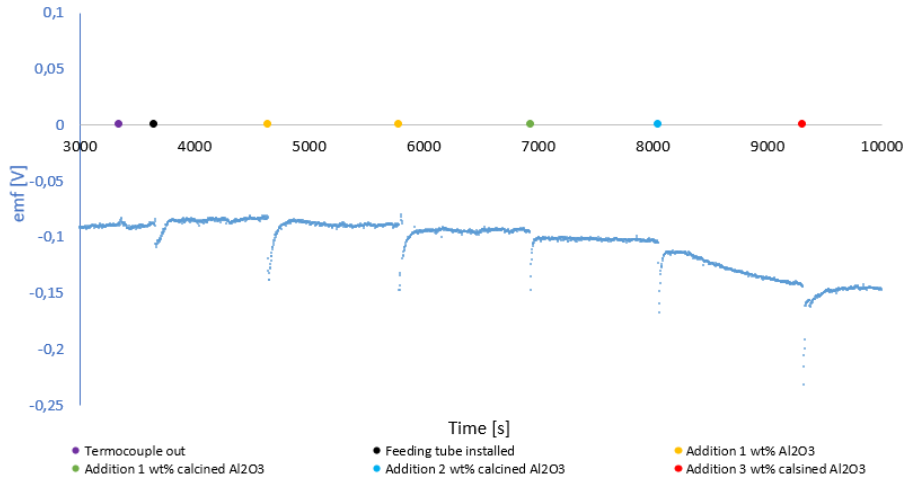

Figure 5.23: Emf between a totally immersed graphite electrode and the graphite reference. Portions of 1 wt% primary alumina (yellow data point) and portions of fully calcined alumina (green=1 wt%, blue=2 wt%, red=3 wt%) were added. The purple data point is removal of the thermocouple and the black data point are installation of the feeding tube. Nitrogen was bubbled into the melt during the experiment.

By studying the changes in potential between the totally immersed electrode and the graphite reference it can be seen that the emf is reduced with approximately 0.01 V each time 1 wt% Al_2O_3 is added (in the time interval 5000-8000s). A drop in emf of 0.01 V is equivalent to a change in activity of oxide of 20 % ($a_{after\ addition}/a_{before\ addition}$=1.20). This is not too different from the theoretical values calculated in FactSage, shown in Figure 2.5, especially not when assuming some alumina in the bath before the first addition. An increase from 1 wt% Al_2O_3 to 2 wt% Al_2O_3 is equivalent to a change in oxide activity of 80 %, while an increase from 2 wt% Al_2O_3 to 3 wt% Al_2O_3 is equivalent to a change in oxide activity of 40 % and an increase from 3 wt% Al_2O_3 to 4 wt% Al_2O_3 is equivalent to a change in oxide activity of 25 %, so this theory seems it fit better for a bath containing some wt%s alumina.

5.10 Addition of Aluminium

In the very end of experiment 4 approximately 0.5 g of solid aluminium was added to the melt. This was done to see how aluminium affected the measurements since, as described earlier, aluminium leak for the reference are believed to affect the emf measurements. The emf drops with about 0.40 V in the moment aluminium

is added. This result gives substance to the argument that the system is sensitive to metal in the bath and that the changes in the melt might take place after very short time. This drop can be due to several reactions. Aluminium may react with sodium fluoride as described in equation (5.1) or with CO_2 or CO. Both dissolved sodium and dissolved aluminium are formed when aluminium is in contact with molten cryolite, as shown below [24].

$$Al(l) + 3NaF(l) = AlF_3(diss) + 3Na(g\,or diss), \tag{5.7}$$

According to Ødegard et al. [25] sodium dissolves in cryolite as free Na while aluminium is present as AlF_2^-. The dissolved aluminium may further migrate towards the anode and an oxidation may occur [7]:

$$AlF_2 + 2F^- = AlF_4^- + 2e^-. \tag{5.8}$$

Aluminium may react with CO_2 as show in equation (2.2) or with CO to form solid carbon:

$$2Al(diss.) + 3CO(g) = 2Al_2O_3(diss.) + 3C(s). \tag{5.9}$$

The formed sodium may also react further with CO and CO_2 and the potential at the graphite sensor and thereby the emf will decrease as a result of that.

Another possible reaction that may occur when metal is added to the melt is the formation of hydrogen gas as a the result of reaction between aluminium and water vapour. Hydrogen gas may also be formed if there is any HF gas present in the system. Aluminium will then react with hydrogen fluoride to form hydrogen and aluminium fluoride. In any case, the reaction will be [24]:

$$2Al + 3H_2O = Al_2O_3 + 3H_2. \tag{5.10}$$

The impact of H_2 on the measurements need to be studied further.

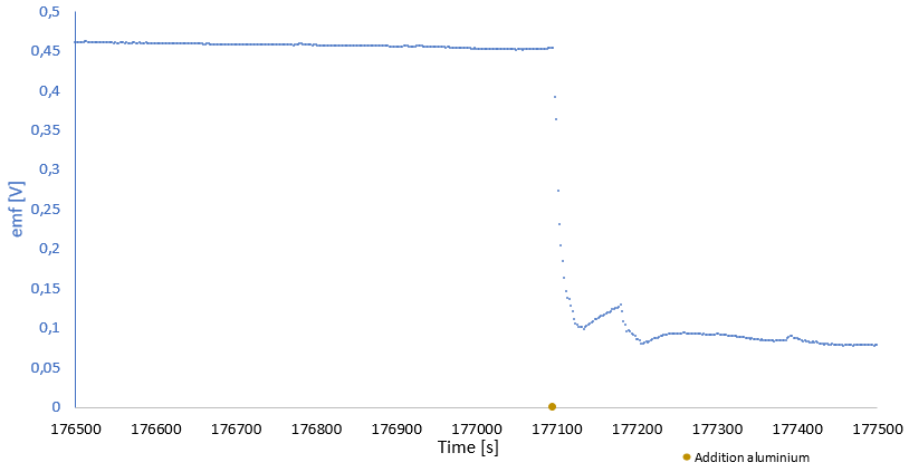

Figure 5.24: Emf between the crucible and the aluminium reference vs time when aluminium is added to the melt.

Chapter 6

Conclusion

Emf measurements between a graphite sensor and two different reference electrodes have been studied in order to figure out if graphite material is suited for determination of alumina concentration in cryolite melts. The system's sensitivity to other variables have been investigated, since it is important that the changes in emf are related to change in alumina concentration and not other variations in the system.

The results showed a decreasing trend in emf values when alumina was added. The total decrease in emf between graphite and the graphite reference electrode was close to what was expected from theoretical calculations when the melt started from an initial alumina concentration of 1 wt% and went all the way to saturation. Since the partial pressure of CO and CO_2 was low and unknown it was impossible to determine exactly how the theoretical emf between the graphite sensor and the aluminium reference electrode would vary, but it showed a logarithmic decreasing trend which was expected according to the Nernst equation. An important observation from the initial experiments was that it was observed sudden drops and jumps in emf immediately after addition. A large part of the following work was dedicated to reveal the reasons for this behaviour.

It is evident that the system is sensitive to other changes than variations in alumina concentration. Introduction of CO_2 gas gave substantial impact on the emf, so the assumption of a constant partial pressure of CO/CO_2 used in the theoretical calculations might not be valid, and a solid buffer system of CO/CO_2 may be needed to reduce the influence of variation in the partial pressures of CO and CO_2. However, the sudden drops and jumps in the potential after alumina addition were

still present even though CO_2 was fed to the system.

It seemed like gas evolution caused by the reaction between moisture or hydoxyl containing species in the primary alumina in conjunction with the addition of primary alumina affected the emf immediately after addition, but the effect was reduced by the use of fully calcined alumina and a totally immersed probe.

Drifting in emf was observed in all experiments and might have several explanations. The reaction between dissolved metal, possibly stemming from the aluminium reference electrode, and CO and CO_2 is believed to be one of the main reasons for the drifting. To get the aluminium leakage from the aluminium reference electrode under control and to develop a solid buffer system of CO and CO_2 seem important.

The use of graphite sensors for determination of alumina concentration in cryolite melts is not appropriate as long as other variations in the system influence the measured potentials. To get control of the other variables in the system will be important in the further development of this method of measuring the alumina concentration.

Chapter 7

Further Work

Several experiments could be performed building on this thesis. Some ideas to what could be done further are listed below:

- Design of an aluminium reference electrode without a open hole for electrolyte penetration to hinder leak of aluminium into the bath. One idea might be to use a porous plug e.g. sintered boron nitride or make a boron nitride tube with very thin walls which can act as the diaphragm.
- Run an experiment without using an aluminium reference to avoid the potential problem of aluminium leaking into the crucible compartment to study how aluminium form the reference may impact the emf measured between a graphite sensor and the graphite reference.
- Make a solid buffer system for CO/CO_2. Bubbling of CO gas might be one alternative.
- Study of the gas composition above the melt after addition of alumina.
- Add alumina in the form of liquid melt additions with high alumina content in order to avoid reaction between the melt in the crucible compartment and the primary alumina.

Bibliography

[1] Regjeringen. Business and industry in norway - the metals industry. https://www.regjeringen.no/no/dokumenter/Business-and-industry-in-Norway—The-metals-industry/id419341/. Accessed: 10/05/2018.

[2] K Grotheim and H Kvande. Introduction to aluminium electrolysis-understanding the hall-heroult process. *Aluminium-Verlag. Dusseldorf*, 1993.

[3] Shui-qing Zhan, LI Mao, Jie-min Zhou, Jian-hong Yang, and Yi-wen Zhou. Analysis and modeling of alumina dissolution based on heat and mass transfer. *Transactions of Nonferrous Metals Society of China*, 25(5):1648–1656, 2015.

[4] A Sterten, S Haugen, and K Hamberg. The naf-alf3-al2o3-na2o system—i standard free energy of formation of α-aluminium oxide from emf measurements. *Electrochimica Acta*, 21(8):589–592, 1976.

[5] John W Burgman, James A Leistra, and Paul J Sides. Aluminum/cryolite reference electrodes for use in cryolite-based melts. *Journal of The Electrochemical Society*, 133(3):496–500, 1986.

[6] K Grjotheim, C Krohn, M Malinovsky, K Matiasovsky, J Thonstad, and Aluminium Electrolysis. Fundamentals of the hall–héroult process. *Aluminium Electrolysis*, 2, 1982.

[7] Jomar Thonstad, Pavel Fellner, Geir Martin Haarberg, Jan Hives, H Kvarde, and Asmund Sterten. *Aluminium Electrolysis: Fundamentals of the Hall-Herault Process*. Aluminium-Verlag, 2001.

[8] Kai Grjotheim and Barry J Welch. Aluminium smelter technology-a pure

and applied approach. *Aluminium-Verlag, P. O. Box 1207, Konigsallee 30, D 4000 Dusseldorf 1, FRG, 1980.*, 1980.

[9] Camilla Sommerseth. The effect of production parameters on the performance of carbon anodes for aluminium production, doctorial thesis, ntnu. 2016.

[10] Kai Grjotheim and Barry J Welch. Aluminium smelter technology-a pure and applied approach. *Aluminium-Verlag, P. O. Box 1207, Konigsallee 30, D 4000 Dusseldorf 1, FRG, 1988.*, 1988.

[11] Kenneth R Seecharran. Bayer process chemistry. *Alumina Plant, Guymine, Linden.*, 2010.

[12] L Keith Hudson, Chanakya Misra, Anthony J Perrotta, Karl Wefers, and FS Williams. Aluminum oxide. *Ullmann's Encyclopedia of Industrial Chemistry*, 2000.

[13] Xiangwen Wang. Alumina dissolution in aluminum smelting electrolyte. *Light Metals*, 2009:383–388, 2009.

[14] J Thonstad, A Solheim, S Rolseth, and O Skar. The dissolution of alumina in cryolite melts. In *Essential Readings in Light Metals*, pages 105–111. Springer, 1988.

[15] RG Haverkamp, BJ Welch, S Bouvet, and P Homsi. Alumina quality testing procedure. *LIGHT METALS-WARRENDALE-*, pages 119–126, 1997.

[16] NE Richards, S Rolseth, J Thonstad, and RG Haverkamp. Electrochemical analysis of alumina dissolved in cryolite melts. *LIGHT MET(WARRENDALE PA)*, pages 391–404, 1995.

[17] NV Vasyunina, IP Vasyunina, Yu G Mikhalev, and AM Vinogradov. The solubility and dissolution rate of alumina in acidic cryolite aluminous melts. *Russian Journal of Non-Ferrous Metals*, 50(4):338–342, 2009.

[18] Donald R Sadoway. Aluminum reference electrode, August 16 1988. US Patent 4,764,257.

[19] JW Burgman and J Leistra. A reference electrode for hall cell experiments. *Light Metals 1986.*, 2:463–472, 1986.

[20] A Sterten, K Hamberg, and I Maeland. Activities and phase diagram data of sodium fluoride-aluminum fluoride-aluminum oxide mixtures derived from electromotive force and cryoscopic measurements. standard thermodynamic data of β-aluminum oxide (s), sodium hexafluoroaluminate (s), sodium

tetradecafluorotrialuminate (s), and sodium tetrafluoroaluminate (l). *ChemInform*, 13(30), 1982.

[21] F. Olufsen. Emf-målinger for bestemmelse av endringer i aluminumsfluoridinnholdet i kryolittsmelter, hovedoppgave, ntnu. 1996.

[22] Karen Sende Osen, A Solheim, C Rosenkilde, and Egil Skybakmoen. The behaviour of moisture in cryolite melts. *Light metals*, pages 395–400, 2009.

[23] Margaret Hyland, Edwin Patterson, and Barry Welch. Alumina structural hydroxyl as a continuous source of hf. In *Essential Readings in Light Metals*, pages 936–941. Springer, 2016.

[24] Kai Grjotheim. *Contribution to the Theory of the Aluminum Electrolysis*. I Kommisjon Hos F. Bruns Bokhandel, 1956.

[25] R Ødegård, Å Sterten, and J Thonstad. The solubility of aluminium in cryolitic melts. In *Essential Readings in Light Metals*, pages 39–48. Springer, 2016.

Appendix

A The Relationship between Alumina Concentration and the Activity of Na_2O

Data from FactSage was used to find the relationship between alumina concentration and the activity of Na_2O. This relationship has been used in theoretical calculations of the cell potential.

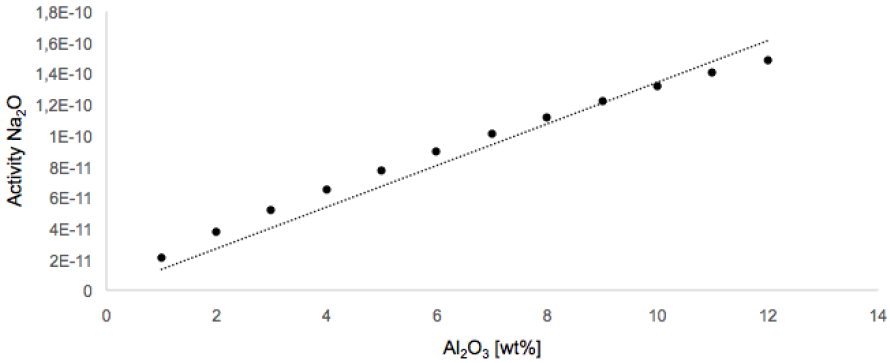

Figure A.1: The relationship between alumina concentration and the activity of Na_2O.

B E^0 for the Aluminium Reference Cell Reaction

The table below show E^0 values for the reaction between a carbon electrode and the aluminium reference electrode at different temperatures.

Table B.1: E^0 values for the reaction between a carbon electrode and the aluminium reference electrode at different temperatures.

Temperature [°C]	E^0 [V]
940	1.0955
950	1.0853
960	1.0751
970	1.0549
980	1.0547
990	1.0445
1000	1.0343
1010	1.0241

C Experiment 2

This section shows the results where the graphite electrode is used as sensor in experiment 2. Figure C.2 shows the emf between the graphite electrode and graphite reference vs time. Figure C.3 shows the emf between the graphite electrode and aluminium reference vs time.

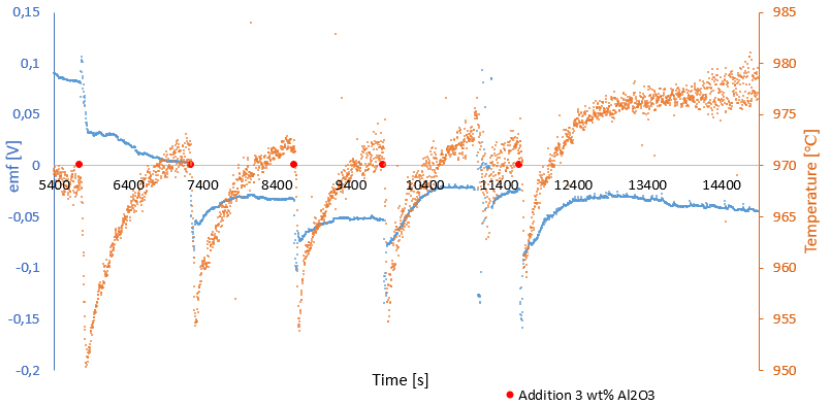

Figure C.2: Emf between the graphite electrode and graphite reference vs time (blue dots) in experiment 2. Temperature vs time (orange dots). The red data points indicate addition of 3 wt% alumina.

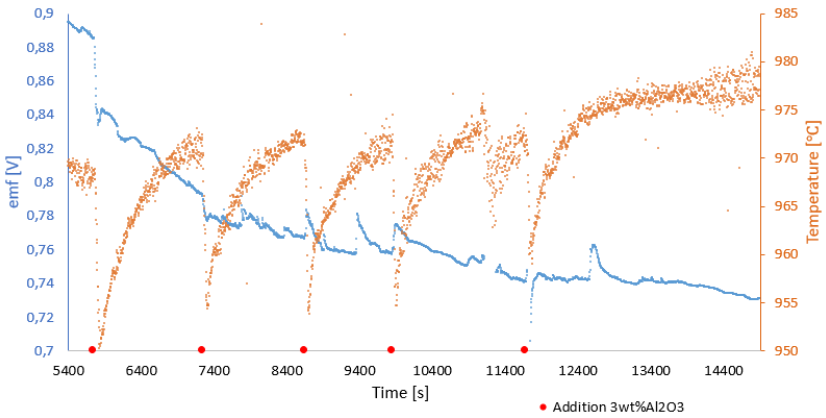

Figure C.3: Emf between the graphite electrode and aluminium reference vs time (blue dots) in experiment 2. Temperature vs time (orange dots). The red data points indicate addition of 3 wt% alumina.

D Experiment 3

This section shows the results where the graphite electrode is used as sensor in experiment 3. Figure D.4 shows the emf between the graphite electrode and graphite reference vs time. Figure D.5 shows the emf between the graphite electrode and aluminium reference vs time.

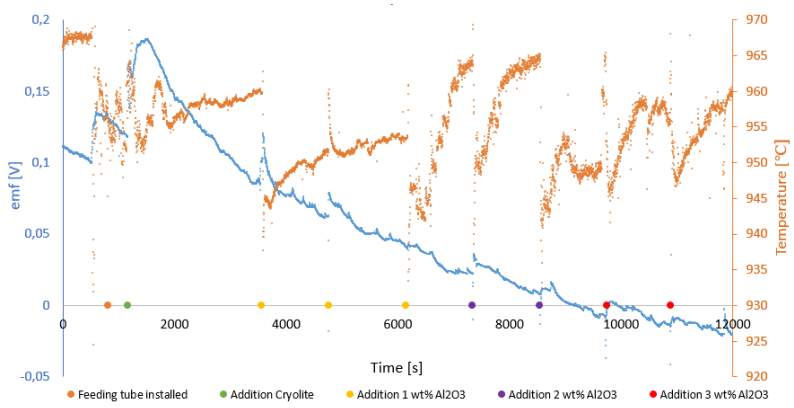

Figure D.4: Emf between the graphite electrode and graphite reference vs time (blue dots) and temperature vs time (orange dots) in experiment 3. The orange data point is installation of feeding tube, the green one is addition of cryolite to the melt. The yellow, purple and red data points are additions of 1 wt%, 2 wt% and 3 wt% of alumina, respectively.

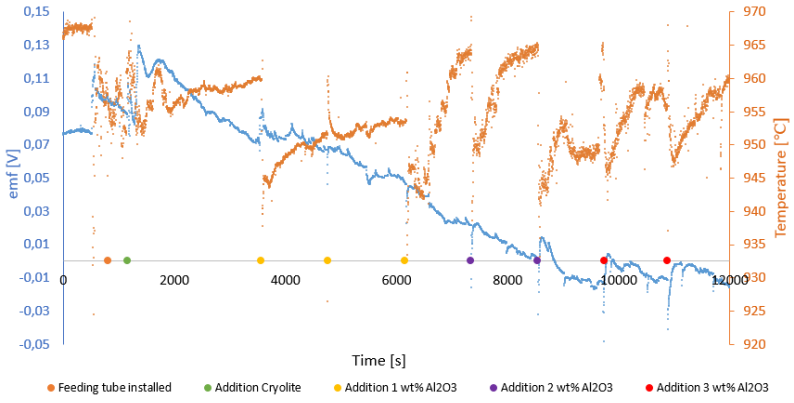

Figure D.5: Emf between the graphite electrode and aluminium reference vs time (blue dots) and temperature vs time (orange dots) in experiment 3. The orange data point is installation of feeding tube, the green one is addition of cryolite to the melt. The yellow, purple and red data points are additions of 1 wt%, 2 wt% and 3 wt% of alumina, respectively.

E Risk Assessment

ID	26991	**Status**	**Dato**
Risikoområde	Risikovurdering: Helse, miljø og sikkerhet (HMS)	Opprettet	15.01.2018
Opprettet av	Karoline Aasen Nilsen	Vurdering startet	19.02.2018
Ansvarlig	Karoline Aasen Nilsen	Tiltak besluttet	
		Avsluttet	

Risikovurdering:

IKP, Master Thesis, Karoline Aasen Nilsen, 2018

Gyldig i perioden:
1/15/2018 - 1/15/2021

Sted:
IKP (IME labs)

Mål / hensikt
This risk assessment contains all the activities that the master student Karoline Aasen Nilsen will perform in the lab regarding her master thesis: Alumina concentration measurements in cryolite melt.

Bakgrunn
The master project aims is to measure the alumina concentration during the whole dissolution process since alumina dissolution is one of the most important processes taking place in the Hall-Heroult process for the production of primary aluminium.

Beskrivelse og avgrensninger

The main goal of the master project is to be able to measure the alumina concentration in such a way that the concentration can be measured during the whole dissolution process. The idea is to design reference electrode that can be used in emf measurements. The laboratory experiments will be performed in a closed high temperature furnace.

Forutsetninger, antakelser og forenklinger
[Ingen registreringer]

Vedlegg
[Ingen registreringer]

Referanser
[Ingen registreringer]

Oppsummering, resultat og endelig vurdering

I oppsummeringen presenteres en oversikt over farer og uønskede hendelser, samt resultat for det enkelte konsekvensområdet.

Farekilde: **Use of dimond saw**

Uønsket hendelse: **Rubble**

Konsekvensområde: Helse — Risiko før tiltak: Risiko etter tiltak:

Uønsket hendelse: **Splach of water**

Konsekvensområde: Helse — Risiko før tiltak: Risiko etter tiltak:
Materielle verdier — Risiko før tiltak: Risiko etter tiltak:

Uønsket hendelse: **Cuts**

Konsekvensområde: Helse — Risiko før tiltak: Risiko etter tiltak:

Uønsket hendelse: **damage to hearing**

Konsekvensområde: Helse — Risiko før tiltak: Risiko etter tiltak:

Farekilde: **Core drill**

Uønsket hendelse: **Rubble**

Konsekvensområde: Helse — Risiko før tiltak: Risiko etter tiltak:
Materielle verdier — Risiko før tiltak: Risiko etter tiltak:

Uønsket hendelse: **Damage to hearing**

Konsekvensområde: Helse — Risiko før tiltak: Risiko etter tiltak:

Uønsket hendelse: **splach of water**

Konsekvensområde: Helse — Risiko før tiltak: Risiko etter tiltak:
Materielle verdier — Risiko før tiltak: Risiko etter tiltak:

Farekilde: **Core drill**

Uønsket hendelse: **Loosening of material**

Konsekvensområde: Materielle verdier — Risiko før tiltak: Risiko etter tiltak:

Farekilde: **High temperature closed furnace**

Uønsket hendelse: **Fire and burns**

Konsekvensområde: Helse — Risiko før tiltak: Risiko etter tiltak:
Ytre miljø — Risiko før tiltak: Risiko etter tiltak:
Materielle verdier — Risiko før tiltak: Risiko etter tiltak:

Uønsket hendelse: **furnace overheating due to water leak or missing cooling water**

Konsekvensområde: Helse — Risiko før tiltak: Risiko etter tiltak:
Materielle verdier — Risiko før tiltak: Risiko etter tiltak:

Uønsket hendelse: **overheating of the furnace due to mispositioned or short fruit of thermocouple**

Konsekvensområde: Ytre miljø — Risiko før tiltak: Risiko etter tiltak:
Materielle verdier — Risiko før tiltak: Risiko etter tiltak:

Uønsket hendelse: **Exposure to dust form hazardous chemicals**

Konsekvensområde: Helse — Risiko før tiltak: Risiko etter tiltak:
Ytre miljø — Risiko før tiltak: Risiko etter tiltak:

Uønsket hendelse: **Electric shock from rectifier/potentiostat**

Konsekvensområde: Helse — Risiko før tiltak: Risiko etter tiltak:

Farekilde: **Muffle furnace**

Uønsket hendelse: **Burn**

Konsekvensområde: Helse — Risiko før tiltak: Risiko etter tiltak:

Endelig vurdering

Involverte enheter og personer

En risikovurdering kan gjelde for en, eller flere enheter i organisasjonen. Denne oversikten presenterer involverte enheter og personell for gjeldende risikovurdering.

Enhet /-er risikovurderingen omfatter

- Institutt for kjemisk prosessteknologi
- Institutt for materialteknologi

Deltakere

Luis Carlos Izaguirre Bracamonte

Espen Sandnes

Gisle Øye

Lesere

Gunn Torill Wikdahl

Eva Rise

Andre involverte/interessenter

[Ingen registreringer]

Følgende akseptkriterier er besluttet for risikoområdet Risikovurdering: Helse, miljø og sikkerhet (HMS):

Helse

Materielle verdier

Omdømme

Ytre miljø

Oversikt over eksisterende, relevante tiltak som er hensyntatt i risikovurderingen

I tabellen under presenteres eksisterende tiltak som er hensyntatt ved vurdering av sannsynlighet og konsekvens for aktuelle uønskede hendelser.

Farekilde	Uønsket hendelse	Tiltak hensyntatt ved vurdering
Use of dimond saw	Rubble	Safety goggles
	Rubble	training for the istrument
	Splach of water	Safety goggles
	Cuts	training for the istrument
	damage to hearing	hearing protection
Core drill	Rubble	Safety goggles
	Rubble	training for the istrument
	Damage to hearing	hearing protection
	splach of water	Safety goggles
	splach of water	training for the istrument
	Loosening of material	Fasten the material before drilling
High temperature closed furnace	Fire and burns	Safety goggles
	Fire and burns	high temperature gloves
	Fire and burns	Face shield
	Fire and burns	training for the istrument
	Fire and burns	Use an extra control termocouple
	Fire and burns	Use fire protection system
	Fire and burns	check of furnace thermocouple position and connections
	Fire and burns	check for cooling water leaks and water flow
	furnace overheating due to water leak or missing cooling water	training for the istrument
	furnace overheating due to water leak or missing cooling water	ensure valves
	furnace overheating due to water leak or missing cooling water	check for cooling water leaks and water flow
	overheating of the furnace due to mispositioned or short fruit of thermocouple	high temperature gloves
	overheating of the furnace due to mispositioned or short fruit of thermocouple	training for the istrument
	overheating of the furnace due to mispositioned or short fruit of thermocouple	Use an extra control termocouple
	overheating of the furnace due to mispositioned or short fruit of thermocouple	Use fire protection system

High temperature closed furnace	overheating of the furnace due to mispositioned or short fruit of thermocouple	check of furnace thermocouple position and connections
	Exposure to dust form hazardous chemicals	gas mask
	Electric shock from rectifier/potentiostat	high temperature gloves
	Electric shock from rectifier/potentiostat	all leafs and connection are insulated
Muffle furnace	Burn	high temperature gloves
	Burn	use tongs

Eksisterende og relevante tiltak med beskrivelse:

Safety goggles
Protects eyes

hearing protection
protects ears

high temperature gloves
[Ingen registreringer]

Face shield
[Ingen registreringer]

training for the istrument
[Ingen registreringer]

Fasten the material before drilling
[Ingen registreringer]

Use an extra control termocouple
[Ingen registreringer]

Fasten material before cutting
[Ingen registreringer]

Use fire protection system
[Ingen registreringer]

ensure valves
[Ingen registreringer]

gas mask
[Ingen registreringer]

check of furnace thermocouple position and connections
[Ingen registreringer]

check for cooling water leaks and water flow
[Ingen registreringer]

all leafs and connection are insulated
[Ingen registreringer]

use tongs
[Ingen registreringer]

Risikoanalyse med vurdering av sannsynlighet og konsekvens

I denne delen av rapporten presenteres detaljer dokumentasjon av de farer, uønskede hendelser og årsaker som er vurdert. Innledningsvis oppsummeres farer med tilhørende uønskede hendelser som er tatt med i vurderingen.

Følgende farer og uønskede hendelser er vurdert i denne risikovurderingen:

- **Use of dimond saw**
  - Rubble
  - Splach of water
  - Cuts
  - damage to hearing
- **Core drill**
  - Rubble
  - Damage to hearing
  - splach of water
  - Loosening of material
- **High temperature closed furnace**
  - Fire and burns
  - furnace overheating due to water leak or missing cooling water
  - overheating of the furnace due to mispositioned or short fruit of thermocouple
  - Exposure to dust form hazardous chemicals
  - Electric shock from rectifier/potentiostat
- **Muffle furnace**
  - Burn

Detaljert oversikt over farekilder og uønskede hendelser:

Farekilde: Use of dimond saw

The dimond saw was used to cut tubs of alumina for the construction of the furnace.

Uønsket hendelse: Rubble

Sannsynlighet for hendelsen (felles for alle konsekvensområder): **Lite sannsynlig (2)**

Kommentar:
[Ingen registreringer]

Konsekvensområde: Helse

Risiko:

Vurdert konsekvens: **Liten (1)**

Kommentar: [Ingen registreringer]

Uønsket hendelse: Splach of water

Sannsynlighet for hendelsen (felles for alle konsekvensområder): **Lite sannsynlig (2)**

Kommentar:
[Ingen registreringer]

Konsekvensområde: Helse

Risiko:

Vurdert konsekvens: **Liten (1)**

Kommentar: [Ingen registreringer]

Konsekvensområde: Materielle verdier

Risiko:

Vurdert konsekvens: **Liten (1)**

Kommentar: [Ingen registreringer]

Uønsket hendelse: Cuts

Sannsynlighet for hendelsen (felles for alle konsekvensområder): **Svært lite sannsynlig (1)**

Kommentar:
[Ingen registreringer]

Konsekvensområde: Helse

Risiko:

Vurdert konsekvens: **Stor (3)**

Kommentar: [Ingen registreringer]

Uønsket hendelse: damage to hearing

Sannsynlighet for hendelsen (felles for alle konsekvensområder): **Svært lite sannsynlig (1)**

Kommentar:
[Ingen registreringer]

Konsekvensområde: Helse

Risiko:

Vurdert konsekvens: **Liten (1)**

Kommentar: [Ingen registreringer]

Farekilde: Core drill

Uønsket hendelse: Rubble

Sannsynlighet for hendelsen (felles for alle konsekvensområder): **Svært lite sannsynlig (1)**

Kommentar:
[Ingen registreringer]

Konsekvensområde: Helse

Risiko:

Vurdert konsekvens: **Middels (2)**

Kommentar: [Ingen registreringer]

Konsekvensområde: Materielle verdier

Risiko:

Vurdert konsekvens: **Liten (1)**

Kommentar: [Ingen registreringer]

Uønsket hendelse: Damage to hearing

Sannsynlighet for hendelsen (felles for alle konsekvensområder): **Svært lite sannsynlig (1)**

Kommentar:
[Ingen registreringer]

Konsekvensområde: Helse

Risiko:

Vurdert konsekvens: **Liten (1)**

Kommentar: [Ingen registreringer]

Uønsket hendelse: splach of water

Sannsynlighet for hendelsen (felles for alle konsekvensområder): **Svært lite sannsynlig (1)**

Kommentar:
[Ingen registreringer]

Konsekvensområde: Helse

Risiko:

Vurdert konsekvens: **Liten (1)**

Kommentar: [Ingen registreringer]

Konsekvensområde: Materielle verdier

Risiko:

Vurdert konsekvens: **Liten (1)**

Kommentar: [Ingen registreringer]

Uønsket hendelse: Loosening of material

Sannsynlighet for hendelsen (felles for alle konsekvensområder): **Svært lite sannsynlig (1)**

Kommentar:
[Ingen registreringer]

Konsekvensområde: Materielle verdier

Risiko:

Vurdert konsekvens: **Middels (2)**

Kommentar: [Ingen registreringer]

Farekilde: High temperature closed furnace

Uønsket hendelse: Fire and burns

Sannsynlighet for hendelsen (felles for alle konsekvensområder): **Svært lite sannsynlig (1)**

Kommentar:
[Ingen registreringer]

Konsekvensområde: Helse

Risiko:

Vurdert konsekvens: **Stor (3)**

Kommentar: [Ingen registreringer]

Konsekvensområde: Ytre miljø

Risiko:

Vurdert konsekvens: **Liten (1)**

Kommentar: [Ingen registreringer]

Konsekvensområde: Materielle verdier

Risiko:

Vurdert konsekvens: **Middels (2)**

Kommentar: [Ingen registreringer]

Uønsket hendelse: furnace overheating due to water leak or missing cooling water

Sannsynlighet for hendelsen (felles for alle konsekvensområder): **Svært lite sannsynlig (1)**

Kommentar:
[Ingen registreringer]

Konsekvensområde: Helse

Risiko:

Vurdert konsekvens: **Liten (1)**

Kommentar: [Ingen registreringer]

Konsekvensområde: Materielle verdier

Risiko:

Vurdert konsekvens: **Middels (2)**

Kommentar: [Ingen registreringer]

Uønsket hendelse: overheating of the furnace due to mispositioned or short fruit of thermocouple

Sannsynlighet for hendelsen (felles for alle konsekvensområder): **Lite sannsynlig (2)**

Kommentar:
[Ingen registreringer]

Konsekvensområde: Ytre miljø

Risiko:

Vurdert konsekvens: **Liten (1)**

Kommentar: [Ingen registreringer]

Konsekvensområde: Materielle verdier

Risiko:

Vurdert konsekvens: **Liten (1)**

Kommentar: [Ingen registreringer]

Uønsket hendelse: Exposure to dust form hazardous chemicals

Sannsynlighet for hendelsen (felles for alle konsekvensområder): **Sannsynlig (3)**

Kommentar:

[Ingen registreringer]

Konsekvensområde: Helse

Risiko:

Vurdert konsekvens: **Liten (1)**

Kommentar: [Ingen registreringer]

Konsekvensområde: Ytre miljø

Risiko:

Vurdert konsekvens: **Liten (1)**

Kommentar: [Ingen registreringer]

Uønsket hendelse: Electric shock from rectifier/potentiostat

Sannsynlighet for hendelsen (felles for alle konsekvensområder): **Svært lite sannsynlig (1)**

Kommentar:
[Ingen registreringer]

Konsekvensområde: Helse

Risiko:

Vurdert konsekvens: **Middels (2)**

Kommentar: [Ingen registreringer]

Farekilde: Muffle furnace

Uønsket hendelse: Burn

Sannsynlighet for hendelsen (felles for alle konsekvensområder): **Svært lite sannsynlig (1)**

Kommentar:

[Ingen registreringer]

Konsekvensområde: Helse

Risiko:

Vurdert konsekvens: **Middels (2)**

Kommentar: [Ingen registreringer]

Oversikt over besluttede risikoreduserende tiltak:

Under presenteres en oversikt over risikoreduserende tiltak som skal bidra til å reduseres sannsynlighet og/eller konsekvens for uønskede hendelser.

Detaljert oversikt over besluttede risikoreduserende tiltak med beskrivelse:

Detaljert oversikt over vurdert risiko for hver farekilde/uønsket hendelse før og etter besluttede tiltak